Charles University in Prague
Faculty of Science

Study Programme: Biochemistry
Study Branch: Biochemistry

Bc. Jan Parolek

Evaluace vlastností polymerních konjugátů specificky vážících proteiny pro použití v molekulární biologii

Evaluation of the properties of polymer conjugates which specifically bind proteins and can be used in molecular biology

Diploma Thesis

Supervisor: Doc. RNDr. Jan Konvalinka, CSc.

Consultant: Mgr. Tomáš Knedlík

Prague 2015

Herein I confirm that this thesis was done independently under the supervision of Dr. Jan Konvalinka and that all used literature was properly referenced.

(Prohlašuji, že jsem tuto diplomovou práci vypracoval samostatně pod vedením školitele doc. Jana Konvalinky a že jsem všechny použité prameny řádně citoval.)

Prague, 5th May 2015

……..

Jan Parolek

Acknowledgements

First of all, I would like to give many thanks for my supervisor Jan Konvalinka for accepting me to his research group. He was always very wise teacher to me, and not only in research, but also in terms of attitude to life generally.

Tomáš Knedlík has my huge gratitude, for he guided me in Jan's laboratory since I have started to do there my bachelor thesis. In this point, it is also necessary to thank his wife Veronika, for her patience while Tomáš has been revising my manuscripts.

I would like to thank Pavel Šácha for developing of iBodies project into such greatness, Jan Tykvart for the SPR method mentoring, Michal Svoboda for Ddi1-HisTag preparation, Jana Starková for help with cultivation of mammalian cells, and Jana Pokorná and Milan Kožíšek for help with enzyme inhibition measurements.

I also thank all members of our laboratory for creating a nice working environment where one could work with pleasure.

Department of Biochemistry

Faculty of Science

Charles University in Prague

IOCB AS CR

Institute of Organic Chemistry and Biochemistry, v.v.i.

Academy of Sciences of the Czech Republic

This work was supported by Grant No. P208-12-G016 (Center of Excellence) from the Grant Agency of the Czech Republic and InterBioMed project LO 1302 from the Ministry of Education of the Czech Republic.

Abstract

During last three decades, a great effort was invested to the development of polymer conjugates of low molecular drugs with the aim to improve the specific targeting of drugs to diseased tissues, cells and organs. The main reason for this effort was the fact that high molecular weight copolymers have a favourite distribution profile in tissues and organisms. A linker between a polymer backbone and drug has very important role: it is possible to synthesize a biodegradable linker, which can be enzymatically hydrolyzed. Conversely, there is a possibility to synthesize an inert linker, resistant to the hydrolysis. Proper choice of the suitable precursor-polymer is also essential, hence it has to accomplish all of the stringent demands for biocompatibility. Macromolecular polymer-drug conjugates tend to accumulate in solid tumors because of the so called enhanced permeability and retention (EPR) effect.

There is a whole range of possible applications of high molecular polymer-drug conjugates. In the introduction part of this thesis, I summarize potential use of drugs based on poly(*N*-(2-hydroxypropyl)methacrylamide) (HPMA) copolymers. Moreover, I introduce some therapeutically important proteins used in experimental drug discovery.

In our laboratory, we have developed a concept of HPMA copolymers containing a targeting group (specific inhibitor), an affinity anchor (biotin), and a reporter group (fluorescent label). As a target for the analysis of these conjugates we chose several therapeutic targets, namely glutamate carboxypeptidase II (prostate carcinoma cell membrane marker), HIV-1 protease, and pepsin. Due to their specific properties, we denominated our HPMA copolymer conjugates “iBodies”, a conjunction of an “inhibitor” and “antibodies”.

The enzyme inhibition assays and binding constant determination by surface plasmon resonance revealed that attachment of inhibitor molecules to the copolymer macromolecule preserves binding properties of the inhibitors. iBodies were then used for efficient isolation of all above mentioned proteins from cell lysates. Finally, iBodies were successfully used along with anti-GCPII antibodies in confocal microscopy and flow cytometry. The results prove that iBodies can serve as a fully synthetic substitution of antibodies.

Key words: HPMA conjugates, glutamate carboxypeptidase II, HIV-1 protease, antibody mimetics, protein targeting

(v angličtině)

Abstrakt

V posledních třech desetiletích bylo vloženo značné úsilí do vývoje polymerních konjugátů nízkomolekulárních léčiv. Hlavním důvodem této snahy byla skutečnost, že vytvořené makromolekulární konjugáty mají nejen výhodnější distribuční profil než původní nízkomolekulární léčivo. Při konjugaci má zásadní roli molekulární spojka mezi páteří polymeru a léčivem: spojku je možné vytvořit buď enzymaticky rozložitelnou, nebo odolnou vůči degradačním enzymům. Výběr správného polymerního nosiče je taktéž klíčový, neboť musí splňovat přísné požadavky na biokompatibilitu. Vzniklé makromolekulární konjugáty mají tendenci se akumulovat v solidních nádorech díky efektu nazývanému EPR („Enhanced Permeability and Retention“ efekt).

V praxi existuje řada možností využití makromolekulárních konjugátů nízkomolekulárních léčiv. V úvodu této práce jsem shrnul různé práce o kopolymerech poly(*N*-(2-hydroxypropyl)metakrylamidu (HPMA). V této části práce jsem též stručně představil proteiny experimentálně používané v terapii.

Vyvinuli jsme HPMA kopolymery obsahující cílící ligand (inhibitor), afinitní kotvu (biotin) a signalizační prvek (fluorescenční skupina). Pro testování našich HPMA kopolymerů jsme vybrali následující terapeuticky významné proteiny: glutamátkarboxypeptidasa II (membránový marker karcinomu prostaty), HIV-1 proteasa a pepsin. Vzhledem k jejich specifickým vlastnostem jsme naše HPMA kopolymery pojmenovaly “iBodies”, což je složenina anglických slov “inhibitor” a “antibodies”.

Měření enzymové inhibice a stanovení vazebné konstanty metodou SPR dokázala, že kovalentní připojení molekuly inhibitoru na makromolekulu kopolymeru zachová inhibiční efekt. iBodies byly úspěšně použity k izolaci všech výše zmíněných proteinů z buněčných lyzátů. Nakonec byly iBodies úspěšně použity spolu s monoklonální protilátkou proti GCPII při konfokální mikroskopii a průtokové cytometrii. Výsledek této práce potvrzuje, že iBodies mohou sloužit jako plně syntetická náhrada protilátek.

Klíčová slova: HPMA konjugáty, glutamátkarboxypeptidasa II, HIV-1 proteasa, mimetika protilátek, specifické směřování na proteiny

(In English)

Table of contents

1. Introduction

1.1.HPMA copolymers

The pioneering research of copolymers of poly(*N*-(2-hydroxypropyl)methacrylamide) (HPMA) began in the 1960s, during the quest for suitable hydrophilic biomedical polymer. In the beginning, large number of compounds based on methacrylic acid was tested. Only a few compounds has fulfilled all of the demands for the biocompatibility, polymerization kinetics, stability, possibility of secondary chemical modification, solubility, low immunogenicity, and so forth. Among these, polymers of HPMA had favorable properties, and they represent the most studied group of copolymer-drug carriers [1-3] **(Fig. 1**).

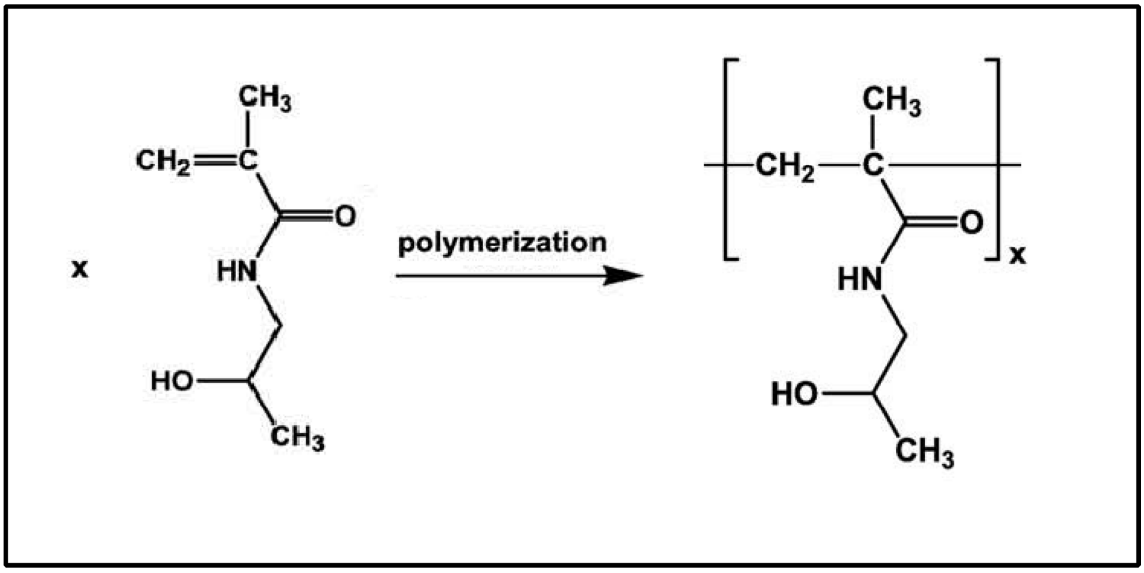

Figure 1: Monomer and polymer of *N*-(2-hydroxypropyl)methacrylamide. HPMA polymers have *N*-substitued hydroxypropyl group, whereas HPMA copolymers have various substitutions in the same position. Adapted from [3].

In 1974, Kopeček *et al.* synthesised *N*-substituted methacrylamides that contained an oligopeptide sequence covalently bound to the polymer backbone. They also described the application of these copolymers as carriers of biologically active compounds [4, 5].

Later on, it was also shown that HPMA copolymers possess low immunogenicity and have very favorable properties for the drug delivery application. [6].

In an effort to specifically target the polymers, Říhová *et al.* tested copolymers possessing two functional groups on a polymer. The first one was the covalently-linked monoclonal antibody against T lymphocytes, the other was cytotoxic agent (daunomycin), linked to the copolymer backbone *via* an enzymatically degradable oligopeptide linker. The complex of antibody-polymer-drug showed high selectivity and effectiveness in *in vitro* tests with murine T lymphocytes. Favourable results were also observed in mice models [7, 8] *in vivo.*

1.2. Physicochemical and biological properties of HPMA copolymers

As described in the previous chapter, HPMA copolymers were chosen because of their very favorable properties *in vivo*. Typical size of these molecules is 5-20 nm. HPMA polymers do not possess a surface charge, which usually acts as the strong attractant for the immune system. Polymer backbone of HPMA copolymers is resistant to hydrolysis, and the copolymers are thus rather stable *in vivo*. Another advantage is that conjugated drugs can be made cleavable from the polymer backbone in lysosomes [2].

Macromolecules are internalized inside the cells by endocytosis. This process can be either non-specific or specific *via* the interaction with particular molecules on the cell surface. After an endosome is formed, it fuses with a lysosome; thereby the intravesicular macromolecules are exposed to the conditions with a high activity of various hydrolases. Novel methods of incorporation an oligopeptide linker has led to the development of HPMA copolymers which can release a conjugated drug enzymatically. Thus, the specificity of the drug effect can be notably increased [2, 9].

Macromolecular nature of HPMA-drug copolymers grants them different distribution profile compared to the original drug. Changed pharmacokinetics can be a useful tool, for example, when the drug release occurs after the internalization in lysosomes inside the cell. In certain cases, the acquired resistance of malignant tumors can be overcome by this approach [10]. Furthermore, HPMA copolymers tend to accumulate in tumors due to the enhanced permeability and retention effect (EPR, see **p. 4**).

The main aspect of the HPMA copolymers elimination is the size of the conjugate. Copolymers smaller than approximately 40 kDa are excreted by the kidney. Copolymers larger than the renal exclusion limit (approx. 45 kDa) are eliminated by biliary excretion [11].

1.3. Enhanced permeability and retention effect (EPR effect)

A major problem of the conventional anticancer chemotherapeutic drugs has been always the lack of selectivity towards the tumor tissue. In 1986, Maeda and Matsumura studied the aberrancies of tumor vasculature and discovered a phenomenon, which was later named as the enhanced permeability and retention (**EPR**) effect [12]. They showed that the blood vessels present in solid tumors are very permeable and, compared to the other tissues, various labeled proteins accumulate inside these tumors. Furthermore, they observed very low recovery of the interstitial fluid from solid tumors to blood or to lymphatic vessels. In the end, they have suggested the EPR effect as relevant for the further development of anticancer agents. They originally called this phenomenon as the tumoritropic accumulation of proteins; however, it became known as the EPR effect [12].

The EPR effect is caused by the abnormal architecture of the blood vessels in solid tumors. Comparing to the normal vasculature, the tumor vasculature presents numerous malformations, *e.g.* vessels lack the smooth muscle layer, the endothelial cells manifest very wide fenestration, the lymphatic drainage is non-effective and the innervation is usually absent. All these disorders are caused by the need of tumors to create precipitously a new way for the nutrition as they become bigger and diffusion is not the sufficient way to supply [13].

Defect blood vessels created during the tumor angiogenesis are responsible for the high vascular permeability, and together with the insufficient lymphatic drainage, macromolecules simply tend to accumulate in solid tumors. The EPR effect is typically observed for macromolecular or lipid agents (liposomes). These macromolecules are accumulated in tumor tissue much more than in the normal tissue [13].

A copolymer of styrene and maleic acid conjugated to the antitumor protein neocarzinostatin, known as SMANCS, is the first copolymer agent with anticancer activity. It was developed in 1979 by Maeda *et al*. The original purpose of neocarzinostatin conjugation to a copolymer backbone was to extent its short *in vivo* half-life. This approach was successful: plasma half-life of the conjugate was ten times longer, and it possessed much lower antigenicity and toxicity compared to the neocarzinostatin itself. Furthermore, the conjugation significantly enhanced the tumoritropism compared to neocarzinostatin [14]. In addition, this research initiated a further examination of the tumoritropism and paved the way for the EPR effect characterization in 1986 by Matsumura and Maeda [12, 13].

1.4. HPMA copolymers as anticancer agents

A plethora of studies on the EPR effect, HPMA copolymers and anticancer therapy has been performed, although most of them were not successful due to the lack of tumor-specific toxicity. Although not every HPMA-drug copolymer was successful, considerable amount of valuable knowledge could be obtained from these studies.

1.4.1. Doxorubicin-HPMA copolymer conjugate PK1

HPMA copolymer composed of doxorubicin covalently bound to the polymer backbone by an oligopeptide linker, named as PK1 (or FCE28068), was the first patented polymer-drug agent. The oligopeptide linker (Gly-Phe-Leu-Gly) is lysosomally cleavable, whereas in the blood stream it remains stable. Doxorubicin was meant to be released intratumorally, due to a higher endocytic and enzymatic activity of a tumor and, of course, due to the EPR effect. The molecular weight of PK1 is 28 kDa and it contains 8.5 % (w/w) of doxorubicin (**Fig. 2, p. 6**) [15].

Doxorubicin is a semisynthetic drug used in cancer chemotherapy. It interferes the DNA functions by intercalating between the bases. This compound is commonly used for the treatment of various cancers, *e.g.* hematological malignancies, solid tumors, and soft tissue sarcomas. Common adverse effects of doxorubicin chemotherapy are hair loss, myelosuppression, nausea and vomiting, and so forth [16].

PK1 was the first synthetic polymer conjugate that entered phase I (in 1994). During the phase I clinical and pharmacokinetic study it was found out, that the doxorubicin conjugated to HPMA possesses more favorable properties: PK1 exhibited no cardiotoxicity and other severe side effects compared to the treatment with free doxorubicin. Output of the phase I was the recommended dose of 280 mg/m^2 every 3 weeks for the phase II [15].

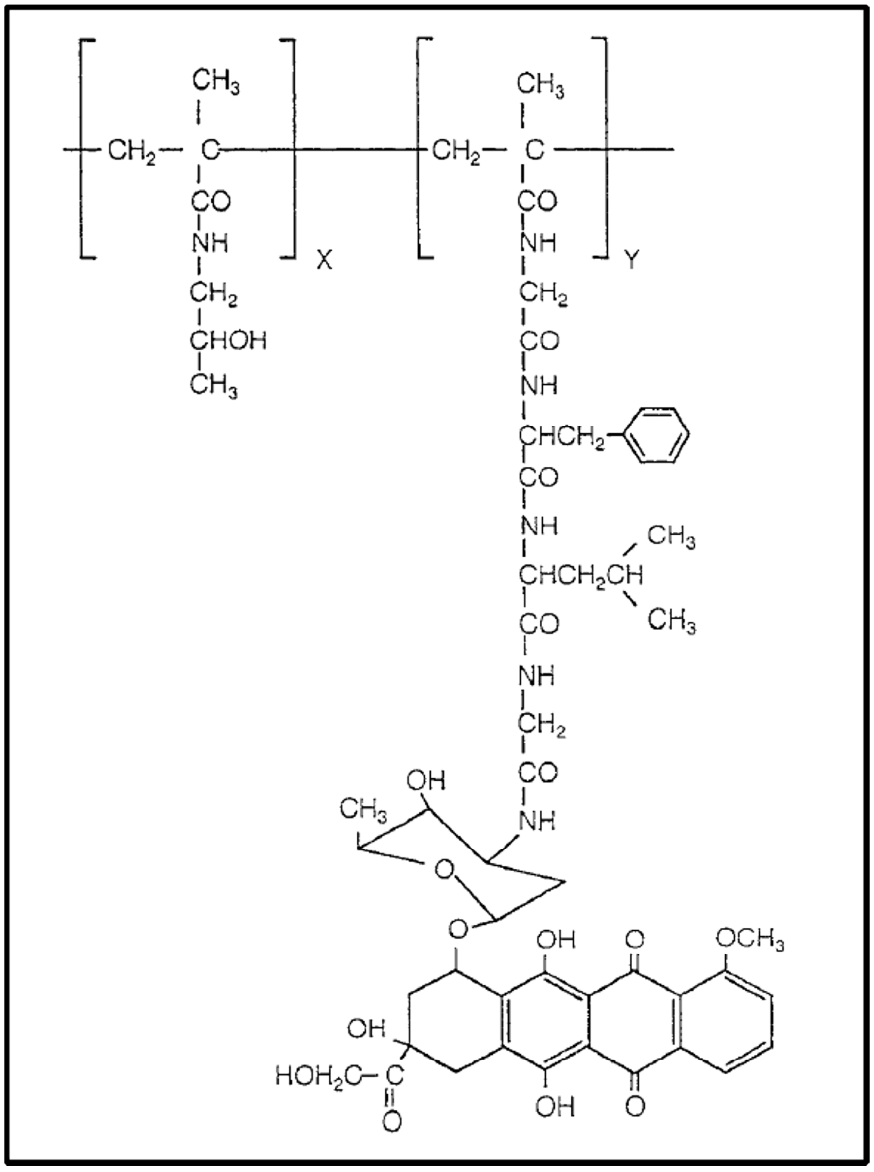

Figure 2: Structure of the conjugate PK1. Doxorubicin is bound to the HPMA backbone by a linker that could be cleaved by lysosomal cathepsins (Gly-Phe-Val-Gly). Adapted from [15].

Following the phase I, phase II of PK1 was published in 2009 by Seymour *et al*., who suggested application of PK1 for breast and non-small cell lung cancer [17]. To date, no further results were published since the phase II of PK1.

1.4.2. Platinum-containing HPMA copolymer conjugate AP5280

Gianasi *et al.* did the first research aimed at comparing of treatment by HPMA copolymer platinates with the treatment by free cisplatin. They focused at drug releasing, toxicity and antitumor activity. Compounds of platinum were bound to the HPMA backbone *via* various biodegradable linkers. Authors reported decreased toxicity (5-15-fold), improved antitumor activity and they marked an opportunity to overcome the platinum resistance of tumor tissue [18].

Following research of HPMA polymer-conjugated platinum was carried out by Bouma *et al.*, Lin *et al.*, and Rademaker-Lakhai *et al.*; compound of their interest is named as AP5280 [19-21]. In this conjugate, there is platinum *N,O*-Pt chelated at the distal end of a cleavable tetrapeptide linker, which is covalently bound to the HPMA backbone (**Fig. 3)**. AP5280 has a molecular weight of approximately 25 kDa and it contains 8.5 % (w/w). Due to the EPR effect, it tends to accumulate in solid tumors. Platinum is then released intratumorally by a lysosomal cysteine proteases, which are present in tumors at a higher rate. In addition to the accumulation in solid tumors, platinum is in this form released slowly and gradually. The compound entered the Phase I study in 2004. Output of the Phase I was the recommended dosing for the Phase II (3300 mg Pt/m^2 once every 3 weeks) [21]. Since 2004, there are not published any further results of AP5280-testing.

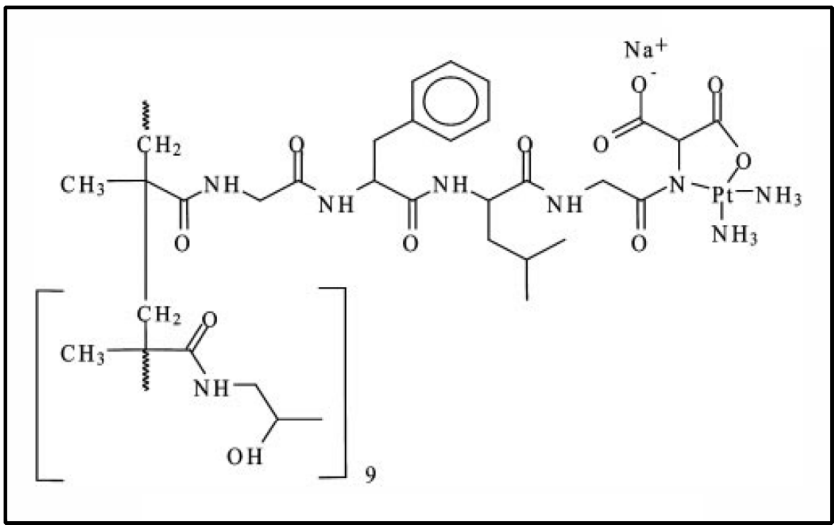

Figure 3: Schematic structure of AP5280. Platinum is chelated to the HPMA backbone by a cleavable linker (Gly-Phe-Leu-Gly). Adapted from [21].

1.4.3. Caplostatin

The first HPMA copolymer conjugate with anti-angiogenic effect is called Caplostatin. It contains fumagillol (TNP-470), covalently bound to the HPMA polymer backbone (**Fig. 4A**). The reason for the preparation of the high molecular conjugate was the toxicity caused to the brain. Conjugation of TNP-470 to the HPMA polymer prevents the compound from crossing the blood-brain barrier, and so the neurotoxicity of TNP-470 is minimalized. Caplostatin showed very promising results in the preclinical studies [22, 23].

1.4.4. HPMA copolymer-(HA14-1)

Inhibitor HA14 was developed to inhibit the anti-apoptic enzyme Bcl-2. This protein is associated with many types of cancer and is highly upregulated in tumor tissue. Utter disadvantages of HA14 are its inherent toxicity when administered intravenously and poor solubility. These inconveniences were successfully solved by conjugating to HPMA polymer (**Fig. 4B**) [24].

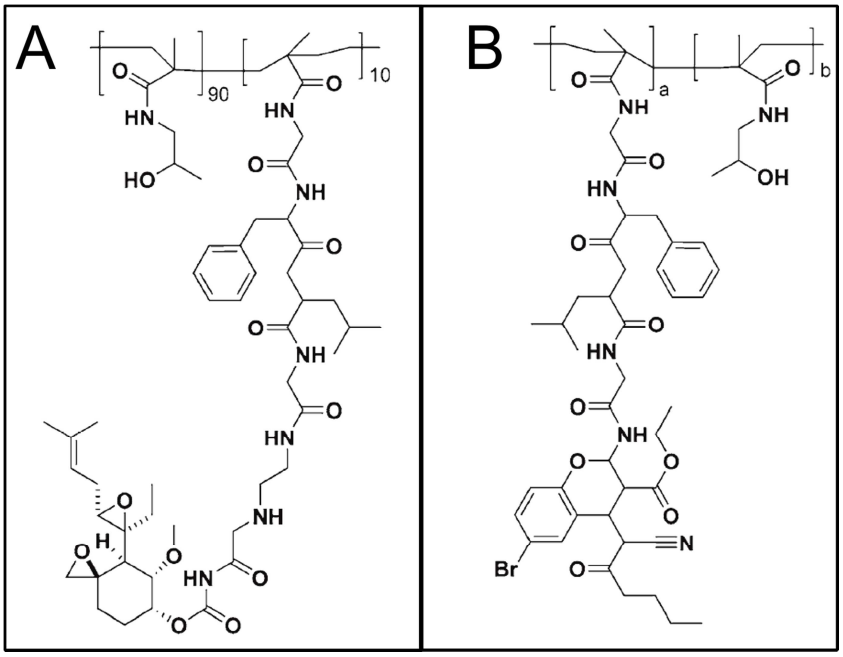

Figure 4: (A) Schematic structure of Caplostatin. TNP-470 is linked with the HPMA backbone by a cleavable linker. **(B) Schematic structure of** . Hydrophobic HA14-1 was conjugated to HPMA backbone by a lysosomally cleavable Gly-Phe-Leu-Gly linker. Adapted from [23].

1.5. Other HPMA-drug anticancer copolymers

PNU166945

Compound name as PNU166945 contains paclitaxel bound to the HPMA polymer backbone and entered the Phase I study. Severe neurotoxic effects at rat models caused the premature discontinuing of the clinical study [25].

PNU166148

Schoemaker *et al.* performed the phase I study on topoisomerase I inhibitor camptothecin linked with the HPMA backbone by a pH-sensitive ester linker. They named this conjugate as PNU166148 (or MAG-CPT) [26]. Bissett *et al.* reported the withdrawal of PNU166148 from clinical development due to the low antitumor effect [27].

1.6. HPMA copolymers at non-cancer therapy

Until now, HPMA copolymer conjugates were in this thesis described only as the anticancer agents. Although the research of HPMA conjugates aimed at non-cancerous diseases treatment is a minor branch of HPMA research, there were done, to date, some remarkable approaches.

1.6.1. Osteoporosis

A number of studies related to HPMA copolymers was performed on bone growth. Pan *et al.* published in 2006 results of experiments on HPMA copolymers consisting of prostaglandin E_1 (PGE_1) bound to the copolymer backbone *via* tetrapeptide spacer sensitive to the cathepsin K. This copolymer contained, besides PGE_1, also an octapeptide of D-aspartic acids, a suitable targeting moiety of agents addressed to the bone tissue [28].

Osteoporosis is a metabolic bone disease which affects usually older people and especially women. It is caused by an imbalance in the uptake and release of the inorganic calcium which form the bone structure. As a result of the calcium insufficiency, bones are fragile and weak, and the sick people are vulnerable to bone fractures. Cells called osteoclasts are mainly responsible for the bone catabolism and their inhibition ceases the degradation process. Cathepsin K is a cysteine protease which is highly expressed by osteoclasts in the bone tissue.

In addition, it is the only known mammalian cysteine protease which is capable of collagen I proteolysis [28, 29].

Prostaglandin E_1 is a potent anabolic agent and causes a considerable increase in the bone anabolism. However, prostaglandins act on various cells *via* their extracellular receptors, and if administered systemically, they are responsible for a variety of side effects. Thus, the prostaglandins were abandoned for some time for the clinical applications [28].

A novel design by Pan *et al.* successfully showed the main advantage of HPMA copolymer Asp_8-PGE_1: there were not seen any of the severe side effects, comparing to the administration of PGE_1. First of all, this HPMA conjugate is accumulated in a bone tissue, due to the calcium-binding octapeptide of D-aspartic acids. When the bone tissue is achieved, the bone-specific protease, cathepsin K, cleaves an oligopeptide linker connecting PGE_1 with the polymer backbone. Subsequently, released PGE_1 is biologically active right in the desired location and with the minimal side effects. After the anabolic dose is achieved, PGE_1 initiates the anabolic processes (**Fig. 5**). In addition, PGE_1 is preferentially released right at the places, where osteoclasts have their activity increased [30, 31].

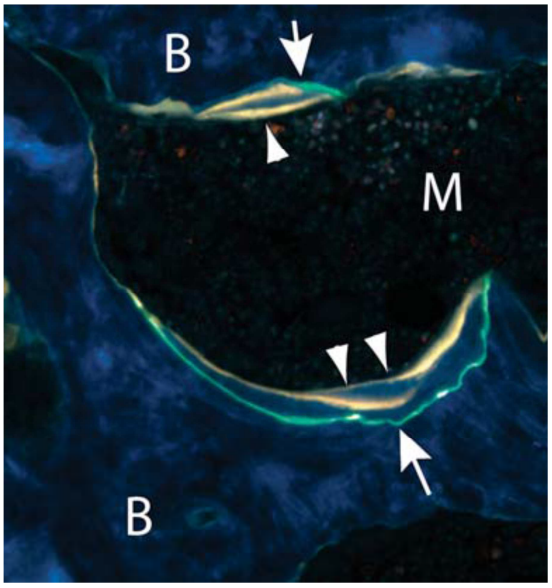

Figure 5: Bone growth caused by HPMA copolymer Asp_8-FITC-PGE_1. The conjugate buried inside the newly grew bone (B) is marked by white arrows and has a green color. New bone formation is detected by a tetracycline marker, in the yellow color and arrowhead markings (M = bone marrow; magnified 250×). Adapted from [30].

HPMA conjugates by Pan *et al*. are smaller than the renal threshold (<~40 kDa), hence they are eliminated from body *via* the renal excretion [28]. Molecules that are smaller than 40 kDa usually undergo the elimination from body too quickly and the therapeutic dosing could be troublesome.

Besides the HPMA copolymer Asp_8-PGE_1, another HPMA copolymer was tested. It is composed of PGE_1 and a different bone targeting moiety, aledronate, a bisphosphonate compound with very high affinity for the bone tissue and with slightly different physiological distribution profile [32].

1.6.2. Rheumatoid arthritis

Rheumatoid arthritis is a chronic systemic inflammatory disease, affecting primarily the joints. The cause of this disease is not totally clear, although many people claim it to be the autoimmune disease. The synovial tissue is described as a primary place of the inflammation. Although there is actually no cure for the rheumatoid arthritis, various anti-inflammatory drugs reduce the symptoms significantly. However, these anti-inflammatory drugs are not specific for the arthritic joints and numerous side effects are often observed [33].

In 2004, Wang *et al.* discovered the accumulation of macromolecules in the arthritic joints. In the beginning, they proved their theory by detection of increased concentration of albumin, using Evans blue dye. Furthermore, they used HPMA copolymer consisted of fluorescein and MRI contrast agent (Gd^{3+} compound). Arthrotropism of the macromolecules is very similar to the EPR effect [33]. By various imaging tools, they were able to show the strong arthrotropism of the macromolecules into the arthritic joints of the adjuvant-induced arthritis rat model [34].

Three years later, Wang *et al.* reported that HPMA copolymer with dexamethasone, an anti-inflammatory steroid compound, connected to the polymer backbone *via* a pH-sensitive linker, improved the condition of ankle joints of the experimental rats with induced arthritis (**Fig. 6, p. 12**) [35]. Further studies were aimed at pharmacokinetic and biodistribution profiles [35, 36]. Later, it was confirmed that this dexamethasone-HPMA copolymer has lowered systemic toxicity [37].

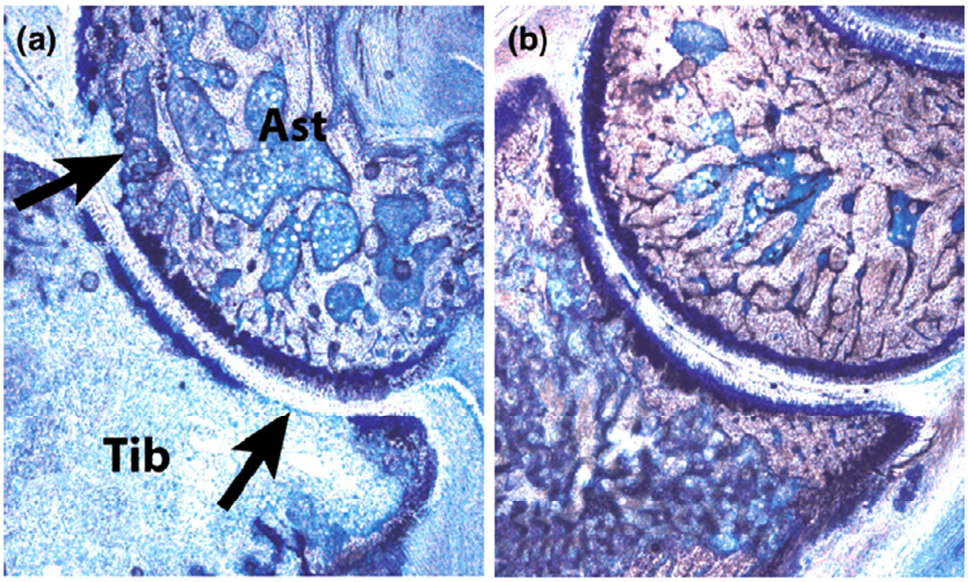

Figure 6: Histological characteristics of the ankle joints from adjuvant-induced arthritis rats. (a) Tibia (Tib) astragalus (Ast) joint from the adjuvant-induced arthritis rats, treated with saline injection. First sample illustrates inflammation, bone loss, and cartilage erosion (arrows). On the other hand, on the picture (b), there is a sample from the adjuvant-induced arthritis rat, treated with HMPA copolymer-dexamethasone. This sample shows intact cartilage and low bone loss. Adapted from [38].

Besides the advantage of local effect, HPMA copolymer-dexamethasone also presents a feature of long-term effect compared to free dexamethasone [35].

1.6.3. Hepatitis B

Jensen *et al.* used HPMA copolymers in hepatitis B virus treatment. They used HPMA copolymer of 21-mer phosphorothioate oligonucleotide and a fluorescent label. Oligonucleotide was the antisense strand to the viral DNA. Moreover, the oligonucleotide was linked with the polymer backbone *via* a degradable oligopeptide sequence. After the oligonucleotide was released into the lysosome, it was translocated to the cytoplasm, and subsequently, into the nucleus. Phosphorothioate oligonucleotides are resistant to the digestion by nucleases, whereas phosphodiester oligonucleotides are cleaved rapidly [39].

Experimental culture of Hep G2 cells, which were incubated with free phosphorothioate oligonucleotide, presented no inhibition of the hepatitis B virus. On the other hand, phosphorothioate oligonucleotide, linked to the polymer backbone *via* cleavable oligopeptide, manifested significant antiviral effect [39].

1.7. Non-HPMA-drug copolymers

1.7.1. Paclitaxel polyglutamate

Compounds derived from paclitaxel conjugated to polyglutamate (PGA) polymer backbone were introduced as the most clinically advanced polymer conjugates with the anticancer effects, *e.g.* paclitaxel poliglumex (**Fig. 7)** [40]. Approximate molecular weight of paclitaxel poliglumex is 38.5 kDa. PGA-paclitaxel compounds have already entered the phase III clinical trials at ovarian cancer. Recommended use was against non-small-cell lung cancer glioblastoma, ovarian cancer, and head and neck cancer [41]. Compared to HPMA copolymers, the main disadvantage of PGA is low solubility in water.

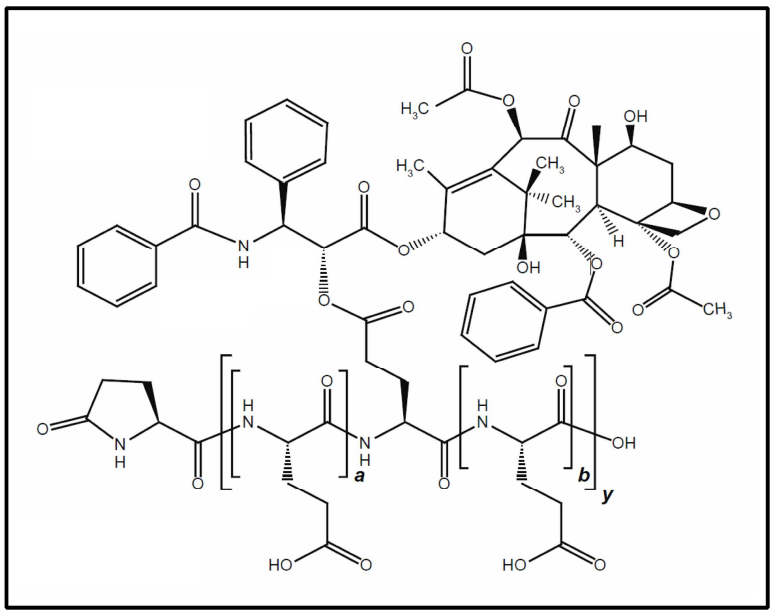

Figure 7: Schematic representation of paclitaxel poliglumex. Paclitaxel is conjugated to polyglutamate polymer backbone by ester linkage to the γ-carboxylic acid side chains of poly-L-glutamic acid. Adapted from [40].

1.8. Possible therapeutic targets

1.8.1. Glutamate Carboxypeptidase II

Glutamate carboxypeptidase II (GCPII) is a homodimeric dizinc metalloprotease, which has a molecular mass of approximately 100 kDa [42, 43] (**Fig. 8**). It is a type II transmembrane protein with extracellular function domain and it exhibits two known physiological functions. First, it cleaves a folylpoly-γ-glutamate in the small intestine, which enables folic acid to be absorbed from small intestine [44]. Second, it hydrolyzes a neurotransmitter *N*-acetyl-L-aspartyl-L-glutamate in the central nervous system, producing two different neurotransmitters, *N*-acetyl-L-aspartate and L-glutamate [45, 46]. Besides these two physiologic roles, GCPII is also expressed in various tissues without any obvious function, namely, in: kidney, lung, salivary gland, ovary, and mostly in prostate [47].

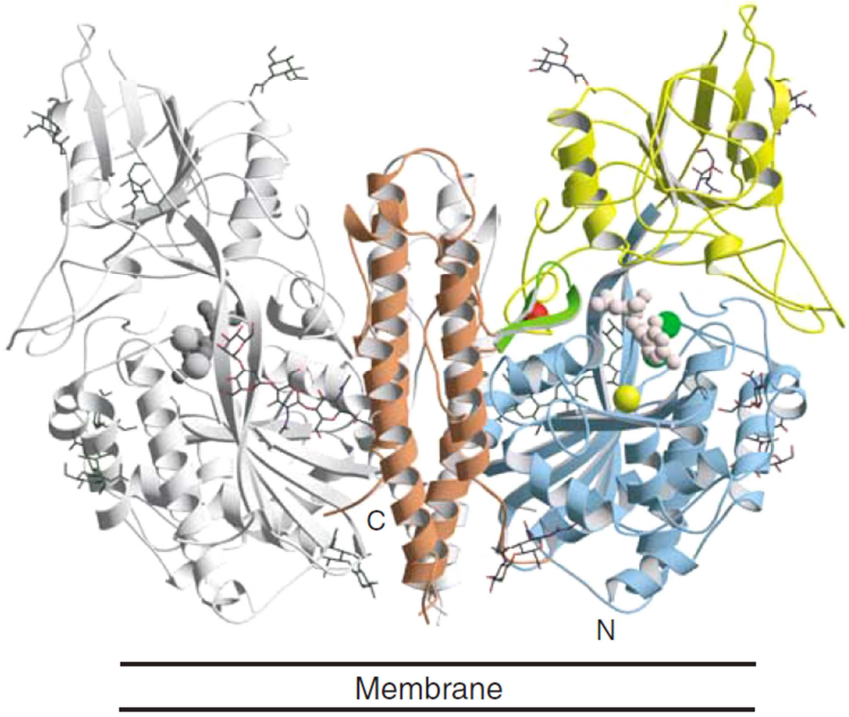

Figure 8: Homodimeric structure of GCPII. One GCPII monomer is shown in grey; the domains of the second monomer are shown in different colors: dimerization domain in brown, apical domain in yellow and protease domain in blue. Ions bound in GCPII structure are represented by spheres: yellow sphere represents chloride ion, red calcium ion and green zinc ion. Adapted from [43].

It was found out that GCPII is highly expressed in the prostate, especially in its cancerous diseases or hyperplasia [48]. Thus, GCPII is used as a diagnostic and prognostic marker for prostate cancer [49]. GCPII is also highly expressed by the neovasculature of solid tumors [50, 51], whereas the physiological neovasculature is GCPII negative [50]. Abundance of GCPII in prostate led to alternative denomination as prostate-specific membrane antigen (PSMA). In addition, the amount of GCPII present in tumor tissue correlates with evaluation by the Gleason score [52]. However, the function of GCPII in prostate is still unknown.

First diagnostic agent, aimed at GCPII, is called ProstaScint. It is an immunoconjugate consisting of ^{111}In conjugate and monoclonal antibody 7E11-C5.3 [53]. After intravenous application of ProstaScint, the area of the cancer presence is displayed by the single-photon emission computed tomography [54].

Very important revelation was the internalization of GCPII *via* clathrin-coated pits [55, 56]. This discovery opened a possibility for GCPII to serve as a drug-delivery target. For example, a monoclonal antibody against GCPII can be conjugated with a cytotoxic molecule by lysosomally cleavable linker, and subsequently, drug release occurs inside the enzyme-rich lysosome [57]. Internalization was also described for the inhibitors of GCPII, which are firmly bound to the extracellular part of the protein [58, 59]. These approaches can be used not only for the eradication of the GCPII positive cells, but also for the various imaging techniques.

1.8.2. HIV-1 protease

Human immunodeficiency virus 1 retropepsin, known better as human immunodeficiency virus 1 protease (HIV-1 PR), is a retroviral aspartic protease. It forms a homodimer which possesses a molecular mass of 21.6 kDa [60, 61]. Its function is essential to the viral life cycle because it produces the infectious viral particles from immature virions. It cleaves viral polyproteins Gag and GapPol, creating the functional virus components, such as nucleocapsid, capsid, and matrix proteins [62]. HIV-1 protease recognizes and cleaves a specifically asymmetrical shape of the peptide substrates, rather than the specific amino acid sequence [63]. This apparent lack of specificity in terms of amino acids preference brought great anxiety to the people who worked on HIV protease substrate specificity [64].

HIV protease represents one of the major targets of anti-HIV therapy (**Fig. 9**). Inhibition of the protease causes a significant viral load reduction in HIV-positive patients. The first protease inhibitor, Saquinavir, was approved by FDA in 1995. Since then nine HIV-1 protease inhibitors was developed and approved. The majority of these inhibitors is derived from the natural substrates or cleavage-sites of HIV protease; inhibitors of this type are often referred to as the peptidomimetics. In fact, a plethora of studies aimed at the inhibitor development made HIV-1 protease one of the most explored enzyme of all times [61, 65].

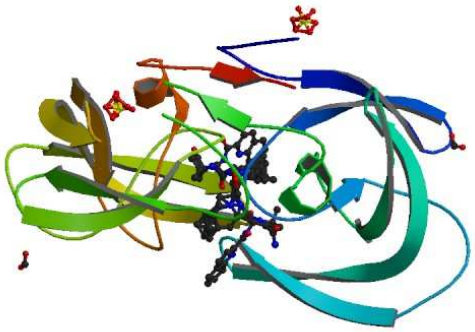

Figure 9: Structure of HIV-1 protease with inhibitor Saquinavir. Dimeric assembly of HIV protease obtained from X-ray crystallography (in resolution of 0.97-1.25Å). Molecule is cocrystallized with formic acid and sulphate ions (PDB.org 3OXC).

2. Aims

Main objective of this thesis is to analyze the potential of HPMA conjugates with low molecular inhibitors of enzymes to replace monoclonal antibodies in a number of biochemical methods.

- To characterize inhibition effect of iBodies towards their target proteins (glutamate carboxypeptidase II, HIV-1 protease, pepsin)
- To test the ability of iBodies to specifically isolate the target protein from cell lysate
- To use iBodies for the imaging and separation of mammalian cells expressing glutamate carboxypeptidase II using flow cytometry and confocal microscopy.

3. Materials

3.1. Chemicals, consumables and other material

Biacore (Sweden)

1-ethyl-3-(3-dimethylaminopropyl)-carbodiimide hydrochloride; *N*-hydroxysuccinimide

Bio-Rad (USA)

Precision Plus Protein™ All Blue Standards to SDS-PAGE; 5× Bio-Rad Protein Assay dye reagent

Fluka (Switzerland)

tetramethylethylendiamine (TEMED); *N*,*N*'- methylenebisacrylamide; sodium citrate

GE Healthcare (UK)

Protein G Sepharose 4 Fast Flow

Gibco (USA)

10% fetal bovine serum (FBS); DMEM-High Glucose medium; RPMI-1640 medium

Hirschmann Gerätte (Germany)

Pasteur pipettes

In Vitro Scientific (California)

4-Chamber 35 mm Glass Bottom Dish

Institute of Photonics and Electronics (Czech Republic)

SPR gold chip

Koh-i-noor Hardmuth (Czech Republic)

transparent 96-well microplate with flat bottom

Lach-Ner (Czech Republic)

silver nitrate; hydrochloric acid; sodium acetate; sodium carbonate; sodium hydroxide; sodium thiosulphate; calcium chloride; ammonium sulphate

Millipore (USA)

0.22 μm nitrocellulose filtration membrane; Amicon Ultra 30 kDa centrifugal filter

Nunc (USA)

white 96-well microplate with conical bottom

P-Lab (Czech Republic)

black 96-well polypropylene microplate with flat bottom

Penta (Czech Republic)

sodium azide; glycerol; hydrogen peroxide; methanol; acetic acid; acetone; formaldehyde; isopropanol; ethyleneglycol; ethanol; formic acid

Pierce Thermo Scientific (USA)

D-biotin; Neutravidin conjugated with horseradish peroxidase; polypropylene 96-well plate (round bottom); NeutrAvidin; SuperSignal West Femto Chemiluminescent Substrate; goat antimouse-IgG antibody conjugated with HRP; goat anti-mouse secondary antibody conjugated with horseradish peroxidase

ProChimia (Poland)

HS-$(CH_2)_{11}$-PEG_4-OH and HS-$(CH_2)_{11}$-PEG_6-O-CH_2-COOH alkanethiols

Roche (Czech Republic)

Protease Inhibitor Cocktail (cOmplete Mini, EDTA-free)

SDT (Germany)

Casein Buffer 20X-4X Concentrate

Serva (Germany)

Coomassie Brilliant Blue G250; bromphenol blue; BSA; ammonium persulfate

Sigma-Aldrich (USA)

Hoechst Stain Solution H34580; ATTO 488 NHS ester; EDTA; SDS; 2-mercaptoethanol; glycerol; glycine; Tris; ethanolamine; acrylamide; boric acid; 2-mercaptoethanol; luminal; Tween-20; KH_2PO_4; NaCl; KCl; HEPES

Solulink (California)

Streptavidin Agarose Ultra Performance

Pharmacia Fine Chemicals (Sweden)

Sephadex G 25

Worthington Biochemical Corporation (USA)

Pepsin

3.2. Instruments

CCD digital camera

ChemiDocIt 600, UVP (Canada)

Cell counter

Countess Automated Cell Counter, Invitrogen (USA)

Centrifuges

Allegra X-15R, Beckman Coulter, Inc. (USA)

Centrifuge 5415R, Eppendorf (Germany)

IEC CL10, Thermo Scientific (USA)

Confocal microscope

LSM 780, Carl Zeiss Microscopy (Germany)

Dounce tissue grinder tube

Working volume 40 ml, Sigma-Aldrich (USA)

Flow cytometer

BD LSR Fortessa™ cell analyzer, Becton Dickinson and Company (USA)

Homogenizer

Emulsiflex-C3, AVESTIN (Canada)

Image scanner

CanoScan 8400F, Canon (Japan)

Incubator

MCO-19AIC CO_2 Incubator, Sanyo (Japan)

Inverted Phase Contrast Microscope

Eclipse TS100, Nikon (Japan)

Laboratory scales

XA 110/X Radwag (Czech Republic)

EK-400H, A&D Engineering, Inc. (USA)

Laboratory shaker

Kisker, (UK)

Microplate reader

Infinite M1000, Tecan (Switzerland)

pH meter

9450, Unicam (UK)

Power supply

PowerPac HC, Bio-Rad (USA)

Sonicator

Elmasonic S30, Elma (Germany)

Spectrophotometer

UNICAM UV500 UV-VIS, Thermo Fisher Scientific (USA)

Surface plasmon resonator (SPR)

Plasmon 4, Institute of Photonics and Electronics in Prague (Czech Republic)

ThermoCellMixing block

MB-102, Bioer (Germany)

Vertical Polyacrylamide Gel Electrophoresis

AP Czech (Czech Republic)

Western blot apparatus

Trans-Blot SD, Bio-Rad (USA)

3.3. Software

BD FACSDiva™ (Becton Dickinson and Company, USA)

Grafit v.7.0.2 (Erithacus, UK)

TraceDrawer 1.5 (Ridgeview Instruments AB, Sweden)

ZEN 2011 (Carl Zeiss Microscopy, Germany).

FlowJo v.10 (FlowJo LLC, USA)

4. Methods

4.1. Design and synthesis of low-molecular-weight compounds and HPMA copolymer conjugates

Tested HPMA copolymers (depicted and summarized in the **Chapter 5.1.**) were prepared by Ing. Jiří Strohalm and Ing. Vladimír Šubr in the laboratory of prof. Karel Ulbrich from the Institute of Macromolecular Chemistry, Academy of Science of the Czech Republic. The low-molecular-weight ligands, which were conjugated with HPMA copolymer, were synthesized by Mgr. Jiří Schimer in the laboratory of Pavel Majer, Ph.D. from the Institute of Organic Chemistry and Biochemistry, Academy of Sciences of the Czech Republic, Gilead Sciences and IOCB Research Center.

4.2. Inhibition of HIV-1 protease with inhibitors and iBodies

The inhibition analyses were performed by spectrophotometric assay using the chromogenic peptide substrate KARVNle*NphEANle-NH_2 [66]. The substrate is derived from the sequence of a natural substrate, contains chromophoric p-nitrophenylalanine, and was prepared by Ing. Mirka Blechová at Institute of Organic Chemistry and Biochemistry of ASCR. When the substrate is cleaved (the cleavage site is marked by an asterisk), the absorbance maximum decreases, which therefore enables to monitor the cleavage by spectroscopy as a decrease of absorbance at 305 nm. Michaelis-Menten constant (K_m), the catalytic efficiency of the enzymes (k_{cat}), and precise concentration of the enzyme (E_0) were determined previously [67]. [S] was 15 µM and K_m was equal to 15 µM.

The 1ml reaction mixture contained 100 mM sodium acetate, 300 mM NaCl, pH 4.7, 6.8 pmol of HIV-1 protease and inhibitor in various concentrations range. Substrate was added to a final concentration of 16 µM. Afterwards, the hydrolysis of substrate was followed as a decrease of absorbance at 305 nm using a UNICAM UV500 UV−VIS spectrophotometer.

Program GraFit 7.0.2 was used for calculation of IC_{50} and K_i values. The K_i value from experimentally obtained apparent inhibition constant (K_i') was calculated using an equation for competitive inhibition according to Williams and Morrison [68]:

$$K_i = \frac{K_i'}{1 + \frac{[S]}{K_m}}$$

4.3. Inhibition of pepsin activity with iBody 3

Inhibition of pepsin activity by iBody 3 was determined using a fluorogenic peptide substrate Abz-Lys-Pro-Ala-Glu-Phe-Nph-Ala-Leu (Abz, aminobenzoic acid; Nph, 4-nitrophenylalanine; a kind gift from laboratory of Michael Mareš, Ph.D. at Institute of Organic Chemistry and Biochemistry of ASCR) according to a method published previously [69]. The substrate contains an Abz group and was prepared by Ing. Mirka Blechová at Institute of Organic Chemistry and Biochemistry of ASCR. Product of hydrolysis was continuously monitored by increase of fluorescence (330 nm excitation; 410 nm emission).

The assay was performed on white 96-well plate with conical bottom, reaction volume was 100 µl. The preincubation mixture contained 92 µl of 100 mM sodium acetate, 300 mM NaCl, 0.1% Tween 20, pH 4.7 (acetate buffer), 2 µl 2.5 ng/ul pepsin, and 1 µl iBody solution in the acetate buffer. This mixture was incubated for 10 minutes at 37 °C. Afterwards, 5 µl of 400 µM Abz-Lys-Pro-Ala-Glu-Phe-Nph-Ala-Leu was added and the product release was continuously monitored on a microplate reader TECAN Infinite M1000 by increase of fluorescence (330 nm excitation wavelength; 410 nm emission wavelength). Furthermore, Michaelis-Menten constant (K_m) and the catalytic efficiency of pepsin (k_{cat}) were determined using a set of reactions of pepsin with substrate.

Program GraFit 7.0.2 was used for calculation of IC_{50} and K_i values. Experimentally obtained apparent inhibition constants (K_i') were calculated into inhibition constants K_i.

4.4. Quantification of iBody 1 binding to GCPII by surface plasmon resonance (SPR)

SPR experiments were performed at room temperature according to a protocol published previously [70]. In a typical experimental setup, mixture (7:3) of HS-$(CH_2)_{11}$-PEG_4-OH and HS-$(CH_2)_{11}$-PEG_6-O-CH_2-COOH alkanethiols (with a final concentration of 0.2 mM was incubated with an SPR golden chip for 1 h at 37 °C. The chip was then rinsed by ethanol, deionized water, and dried with a flow of N_2. Finally, the chip was mounted onto the SPR prism.

After flooding of SPR tubes, the activation of carboxylic terminal groups on the chip surface was performed *in situ* by injecting a 1:1 mixture of 76.68 mg/ml 1-ethyl-3-(3-dimethylaminopropyl)-carbodiimide hydrochloride and 11.51 mg/ml *N*-hydroxysuccinimide in deionized water for 5 min at a flow rate of 20 µL/min. Afterwards, the flow rate was raised to 30 µL/min.

Then, a mixture of monoclonal antibody against GCPII (D2B [70]; 20 ng/µl), and BSA (20 ng/µl) in 10 mM sodium acetate, pH 5.0, was loaded for 8 min. Next, a high ionic strength solution (PBS with 0.5 M NaCl) was used to wash out noncovalently bound molecules, followed by addition of 1 M ethanolamine for deactivation of residual activated carboxylic groups.

Afterwards, an 8 ng/µl solution of recombinant extracellular GCPII in TBS (Avi-GCPII) [71]) was bound to the Neutravidin layer. Finally, iBody 1 solution was applied in four concentrations (2, 4, 8 and 16 nM) in 50 mM Tris, 150 mM NaCl, pH 7.4 for 10 min, followed by injection of pure Tris buffer.

Kinetic curves of binding were fitted using the One-To-One interaction model in program TraceDrawer v.1.5 for obtaining the K_d value.

4.5. Affinity purification of GCPII

LNCaP cells endogenously expressing GCPII were lysed by sonication (3×5 min) in 50 mM Tris-HCl, pH 7.4, 150 mM NaCl, 1% Tween 20, containing Protease Inhibitor Cocktail. After a centrifugation (16000× g, 15 min), the cell lysate was diluted in TBST to a final protein concentration of 0.5 mg/ml (GCPII concentration was approximately 500 ng/ml).

First, 200 nM iBody 1 in 50 mM Tris-HCl, 150 mM NaCl, 0.1% Tween 20, pH 7.4 (TBST), was bound to 50 µl Streptavidin Agarose (volume of 1 ml, room temperature, 30 min). Monoclonal antibody J591 (kindly provided by N.H. Bander, Cornell University, New York) [51] bound to 50 µl Protein G Sepharose (5 µg of J591 in volume of 1 ml, room temperature, 30 min), was used as a positive control. iBody 5 lacking targeting ligand, and blank Protein G Sepharose were used as negative controls. Then, the resin was washed three times with 1 ml of TBST. The washed resin was mixed with 1000 µl of the LNCaP lysate and incubated for 1 h at room temperature (total protein concentration was 1 mg/ml). The resin was washed five times with 1 ml of TBST. Finally, bound GCPII was eluted from Streptavidin Sepharose by adding 50 µl of reducing SDS sample buffer (1×) and heating to 98 °C for 10 min.

4.6. Affinity purification of HIV-1 protease and pepsin from spiked LNCaP lysate

HIV-1 protease and pepsin were isolated from spiked LNCaP cell lysate. LNCaP cells grown on two 100 mm Petri dishes were lysed by sonication (3×5 min) in 2 ml of 50 mM Tris-HCl, pH 7.4, 150 mM NaCl, 1% Tween 20. The homogenate was then centrifuged (16000×g, 15 min) and the supernatant was used in subsequent experiment.

First, 200 nM iBody 2 or 3 in 50 mM Tris-HCl, 150 mM NaCl, 0.1% Tween 20, pH 7.4 (TBST), were bound to 30 µl Streptavidin Agarose Ultra Performance (volume of 1 ml, room temperature, 1 h). iBody 6, which lacks the targeting ligand, was used as a negative control. To block unoccupied biotin-binding sites, the Streptavidin resin was incubated with 1 ml of 2 mM biotin, 100 mM Tris-HCl, 150 mM NaCl, pH 7.2. Afterwards, the resin was washed three times with 1 ml of 100 mM sodium acetate, 300 mM NaCl, 0.1% Tween 20, pH 4.7 (acetate buffer).

The washed resin was mixed with 200 µl LNCaP cell lysate spiked with HIV-1 protease [67] (12 ng/µl; total protein concentration was 1 mg/ml) in the acetate buffer, and incubated for 30 min at room temperature. The resin was washed four times with 1 ml of acetate buffer. Finally, bound HIV-1 protease was eluted from Streptavidin Sepharose by adding 30 µl reducing SDS sample buffer and heating to 98 °C for 10 min. pH of the samples was adjusted by adding 3 µl of 5× SDS-PAGE running buffer.

For pepsin affinity purification, resin samples with pre-bound iBodies were mixed with 200 µl of LNCaP cell lysate spiked with pepsin (pepsin concentration was 100 ng/µl; total protein concentration 1.8 mg/ml) in acetate buffer, and incubated for 5 min at room temperature. The resin was washed three times with 1 ml of acetate buffer. Finally, bound pepsin was eluted from resin by adding 30 µl sample buffer (1×) and heating to 98 °C for 10 min. pH of the samples was adjusted by adding 6 µl of 5× SDS-PAGE running buffer.

4.7. Preparation of *E. coli* lysate containing Ddi1-HisTag:

DNA coding for full-length DNA-damage protein 1 (Ddi1) of *Leishmania major* was synthesized by GenScript and subcloned into pET16b vector for N-terminal hexahistidine tagged fusion protein production (Ddi1-HisTag); the resulting fusion protein Ddi1-HisTag was expressed in *E. coli* BL21(DE3)RIL host cells (performed by Mgr. Michal Svoboda in our laboratory; not published). The *E. coli* cells containing Ddi1-HisTag were resuspended in PBS using Dounce tissue grinder tube and lysed by three passages through EmulsiFlex-C3 high pressure homogenizer at 1200 bar. Afterwards, the product was centrifuged (16000×g, 15 min) and the supernatant was used for further experiments.

4.8. Affinity purification of Ddi1-HisTag from *E. coli* lysate

First, 200 nM iBody 4 in 50 mM Tris-HCl, 150 mM NaCl, 0.1% Tween 20, pH 7.4 (TBST) containing 2 mM $NiCl_2$ was bound to 30 µl Streptavidin Agarose Ultra Performance (Solulink) (volume of 1 ml, room temperature, 1 hour). As negative controls, iBody 5, which lacks the targeting ligand, and blank Streptavidin Agarose were used. To block unoccupied Streptavidin biotin-binding sites, the resin was incubated with 1 ml of 2 mM D-biotin, 100 mM Tris-HCl, 150 mM NaCl, pH 7.2 at 37 °C for 15 min. Afterwards, the resin was washed three times with 1 ml of TBST. The resin was then mixed with 1 ml of Ddi1-HisTag *E. coli* lysate (diluted in TBST to final protein concentration of 325 ng/µl), and incubated at room temperature for 1 h. The resin was washed five times with 1 ml of 25 mM imidazole in TBST. Bound proteins were eluted from the resin by adding 30 µl 1 M imidazole in TBS, and incubation for 15 min at 37 °C.

4.9. Determination of protein concentration

Protein concentration was determined using Bradford protein assay [72] in a transparent 96-well plate. Measurement of all samples was performed in duplicates. As a calibration curve, a concentration range of BSA was used (1.25-20 µg/ml). Absorbance at 595 nm was measured by TECAN microplate reader.

4.10. Sodium dodecyl sulfate-polyacrylamide gel electrophoresis (SDS-PAGE)

Sample buffer:

58 mM Tris-HCl; 5% (v/v) glycerol; 2% (w/v) sodium dodecyl sulphate (SDS); 1% (v/v) 2-mercaptoethanol; 0.02% (w/v) bromophenol blue; pH 6.8

Stacking gel (6%):

250 mM Tris-HCl; 5.84% (w/w) acrylamide; 0.16% (w/w) *N*,*N*'-methylenebis(acrylamide); 0.1% (w/v) SDS; 0.005% (v/v) tetramethylethylenediamine (TEMED); 0.1% (w/v) ammonium persulfate (APS); pH 6.8

Resolving gel (12%):

375 mM Tris-HCl; 11.67% (w/w) acrylamide; 0.33% (w/w) *N*,*N*'-methylenebis(acrylamide); 0.1% (w/v) SDS; 0.001% (v/v) TEMED; 0.1% (w/v) APS; pH 8.8

Running buffer:

250 mM glycine; 25 mM Tris-HCl; 0.1% (w/w) SDS; pH 8.8

Casted gel was placed to a vertical electrophoresis apparatus (AP Czech). Samples were loaded to wells in the gel and resolved by constant voltage of 140 V. Proteins were then visualized either by silver staining or Western blotting

4.11. Silver staining of proteins in polyacrylamide gels

Proteins resolved by SDS-PAGE were visualized by silver staining procedure:

1. *Fixation*:	15 min	12% (v/v) CH_3COOH
		50% (v/v) CH_3OH
		0.02% (v/v) HCHO
2. *Wash*	3 × 3 min	50% (v/v) CH_3OH
3. *Exposure*:	60 s	0.02% (w/v) $Na_2S_2O_3 \cdot 5\ H_2O$
4. *Wash*:	3 × 15 s	deionized water
5. *Impregnation*:	20 min	0.2% (w/v) $AgNO_3$
		0.02% (v/v) HCHO
6. *Wash*:	3 × 15 s	deionized water
7. *Development*:	1 min - 10 min	566 mM Na_2CO_3
		16 µM $Na_2S_2O_3 \cdot 5H_2O$
		0.02% (v/v) HCHO
8. *Stop*:	5 min	12% (v/v) CH_3COOH
		50% (v/v) CH_3OH
9. *Preservation*:		25% (v/v) CH_3OH

Stained gels were scanned by image scanner.

4.12. Western blotting

After SDS-PAGE, proteins from the gel were blotted onto a nitrocellulose membrane (wet blotting: 100 V, 1 hour, in buffer 25 mM Tris-HCl, 192 mM glycine, 10% methanol, 0.1% SDS, pH 8.2). The membrane was then blocked with 1.1% (w/v) casein solution in PBS at room temperature for 1 hour.

For GCPII detection, the membrane was incubated with the primary antibody GCP-04 [73] at 4 ℃ for 1 hour (200 ng/ml; diluted in 0.55% casein solution). The membrane was then washed three times with 137 mM NaCl; 2.7 mM KCl; 10 mM Na_2HPO_4; 1.8 mM KH_2PO_4; 0.05 % Tween 20; pH 7.4 (PBST) and incubated with goat anti-mouse-IgG secondary antibody conjugated with horseradish peroxidase (diluted in PBST 1:25,000).

Finally, the blots were washed three times with PBST to remove unbound antibodies and SuperSignal West Femto Chemiluminescent Substrate (Pierce Thermo Scientific) was applied onto them. Chemiluminiscence was captured by CCD digital camera.

4.13. Fluorescent labeling of monoclonal antibody 2G7

A monoclonal antibody against human native GCPII (2G7; [70]) was labeled with an activated fluorophore ATTO 488 (ATTO 488 NHS ester; Sigma-Aldrich). First, 75 μl of 4.3 mg/ml solution of the antibody 2G7 in PBS was mixed with 1 μl of 1 M $NaHCO_3$, pH 8.3. ATTO 488 NHS ester was dissolved in dry DMSO to concentration of 10 mg/ml. Afterwards, 1 μl of 10 mg/ml ATTO 488 NHS ester solution was mixed with the antibody solution and incubated for 1 h at room temperature. Finally, the fluorophore-antibody conjugate was separated from the free fluorophore using a gel permeation chromatography (Sephadex G 25 column) with TBS as a mobile phase. Fractions containing 2G7-ATTO 488 were pooled and concentrated using Amicon Ultra 30 kDa centrifugal filter.

4.14. Flow cytometry

LNCaP cells (endogenously expressing GCPII) were grown on a 100 mm dish to 90% confluence in RPMI complete medium (containing 10% fetal bovine serum and 4 mM L-glutamine). As a GCPII-negative control, PC3 cells were grown on a 100 mm dish to 90% confluence in DMEM complete medium (containing 10% fetal bovine serum and 4 mM L-glutamine). The media were removed, and cells were washed once with PBS and subsequently incubated in 1.5 ml trypsin/EDTA solution, until all adherent cells were released from the dish surface. Cells were resuspended and transferred into 8 ml of RPMI or DMEM complete medium, centrifuged at 250 ×g for 2 min, and washed with 2 ml PBS. Then, 500 µl of 10% fetal bovine serum in PBS was added to block the cell surface (1 h, 37 °C). The final concentration of the cell suspension was 4×10^6 cells/ml.

Afterwards, 50 µl of cell suspension (containing 2×10^5 cells) was placed into wells of a polypropylene 96-well plate (round bottom) and incubated with 10 nM solutions of iBodies 1 and 5 and 400 nM 2G7-ATTO 488 for 1 h at 37 °C. Cells were washed twice with 200 µl of PBS. Finally, the cell suspension was resuspended in 200 µl of 10% fetal bovine serum in PBS, and a single cell suspension was analyzed with a BD LSR Fortessa™ cell analyzer.

The gates on the side scatter and forward scatter were set to ensure measurement of viable cells, and 10,000 events were measured for each well (voltage 200/270 V). All experiments (all staining agents and both cell lines) were performed in triplicate. Analysis was performed using BD FACSDiva™ Software.

4.15. Confocal microscopy

LNCaP cells, which endogenously express GCPII, were grown in RPMI-1640 medium (Gibco) with addition of FBS (10% final concentration; Gibco). As a negative control, GCPII-negative PC3 cells were used, which were grown in DMEM-high glucose medium with addition of L-glutamine (4 mM final concentration; Gibco) and FBS (10% final concentration). Cells were grown on 4-chamber 35 mm glass bottom dishes.

After three days, iBodies 1 and 5 solutions were added into the media to a final concentration of 20 nM. As a positive control, fluorescently labeled anti-GCPII antibody 2G7 (2G7 ATTO 488) [70] was added to a final concentration of 400 nM. The cells were incubated in the presence of iBodies for 2 h at 37 ℃. Then, the media were removed, a solution of Hoechst 34580 dye was added (0.5 μg/ml solution in PBS), and cells were incubated for 10 min at 37 ℃ to stain cell nuclei. Finally, cells were washed once with 500 μl PBS, fixed 30 minutes in 4 % formaldehyde, and again washed with 500 μl PBS.

Confocal images (pinhole 1 Airy unit) of cells in each chamber were taken with a Zeiss LSM 780 confocal microscope using an oil-immersion objective (Plan-Apochromat 63x/1.40 Oil DIC M27). The fluorescent images were collected at room temperature using 4.5% of the 405 nm diode laser (max. power of 30 mW) for excitation with emission collected from 410 to 585 nm (detector voltage: 850 V) for Hoechst 34580 and 4.0% of the 488 nm argon-ion laser (max. power of 25 mW) for excitation with emission collected from 517 to 534 nm (detector voltage: 870 V) for ATTO 488. All images were taken using the same settings. The microscope was operated and the images were processed with ZEN 2011 software (Carl Zeiss Microscopy).

5. Results

5.1. Design and synthesis of low-molecular compounds and HPMA copolymer conjugates

Low-molecular-weight ligands, which were conjugated with HPMA copolymer (i.e. inhibitors of GCPII, HIV-1 protease and aspartic proteases inhibitors as well as triNTA ligand binding polyhistidine sequence), were synthesized by Mgr. Jiří Schimer in the laboratory of Pavel Majer, Ph.D. from the Institute of Organic Chemistry and Biochemistry, Academy of Sciences of the Czech Republic. The HPMA copolymers and their conjugates with the low-molecular-weight ligands were prepared according to published protocol [74, 75], by Ing. Vladimír Šubr, CSc and Ing. Jiří Strohalm in the laboratory of prof. Karel Ulbrich from the Institute of Macromolecular Chemistry (IMC), Academy of Science of the Czech Republic. After synthesis, the polymer conjugates were purified using gel permeation chromatography and, subsequently, the content of functional groups was determined at IMC.

Structures of all tested compounds and conjugates are depicted in **Fig. 10, p. 34**. Composition of iBodies is summarized in **Table 1, p. 35.** Overview of characteristics of the tested iBodies and their precursors is in **Table 2, p. 36**. Complete structure of all tested iBodies is shown at **Supplementary Figures 1-6 on p. 68-73**.

Tested HPMA copolymer conjugates contain specific targeting ligand (an inhibitor), an affinity anchor, and an imaging probe attached to the polymer backbone (**Fig. 10)**.

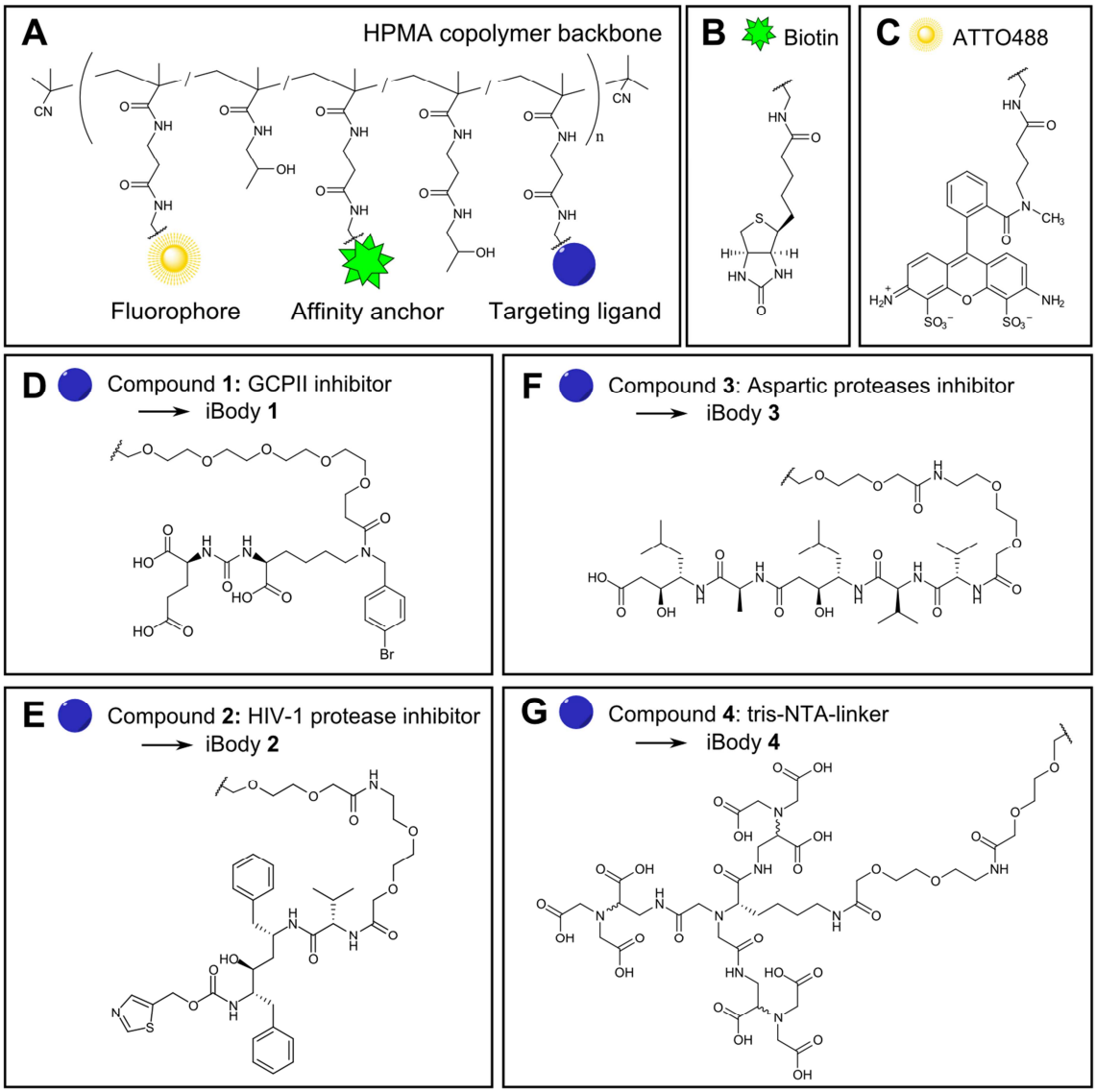

Figure 10: Molecular structures of the tested iBodies. (**A**) Each iBody is composed of HPMA copolymer backbone with covalently attached functional groups – affinity anchor, reporter group and targeting moiety. (**B**) Biotin can be quickly and very firmly immobilized to a number of commercially available resins (*e.g.* Streptavidin Agarose). (**C**) Fluorescent dye ATTO 488 was specially designed for life sciences. (**D**) Compound 1 is a derivative of urea-based GCPII-inhibitor. (**E**) Compound 2, a ritonavir derivative, is potent inhibitor of HIV-1 protease. (**F**) Compound 3, a derivate of pepstatin A, is an inhibitor of aspartate class of proteases. (**G**) Compound 4, containing tris-(nitrilotriacetic) acid, chelates hexahistidine group with nanomolar potency.

Characterization of inhibition effects was determined using a different method for each enzyme. For GCPII, inhibition effect was calculated from SPR-obtained association and dissociation curves (see Methods **p. 24**). In the case of HIV-1 protease, inhibition assay was based on the hydrolysis of chromogenic substrate (see Methods **p. 22**). Pepsin inhibition was determined using a fluorogenic peptide substrate (see Methods **p. 23**). Composition of iBodies is summarized in **Table 1**.

Table 1: Composition of iBodies.

		Number of molecules present in one iBody molecule		
Name	**Targeting**	**Inhibitor**	**Biotin**	**ATTO 488**
iBody **1**	GCPII	Compound **1:** 14	20	5
iBody **2**	HIV-1 protease	Compound **2:** 5	6	-
iBody **3**	aspartic proteases	Compound **3:** 12	15	-
iBody **4**	His-tag sequence	Compound **4:** 10	37	5
iBody **5**	negative control	-	18	6
iBody **6**	negative control	-	13	-

Overview of characteristics of the tested iBodies and their precursors is in **Table 2**.

Table 2: Overview of characteristics of the tested iBodies and their precursors.

Name	**M_r**	**Targeting**	**K_i [pM]**
Compound **22a** [76]	530	GCPII	45 ± 5.7 [76]
Compound **1**	780	GCPII	2,030 ± 430**&**
iBody **1**	106,600	GCPII	3.1 ± 0.5**&**
ritonavir [77]	721	HIV-1 protease	15 ± 2 [77]
Compound **2**	815	HIV-1 protease	12 ± 1
iBody **2**	37,000	HIV-1 protease	7,200 ± 500
acetyl-pepstatin [77]	644	aspartic proteases	116,000 ± 5,000***** [77]
Compound **3**	892	aspartic proteases	623,000 ± 1,700*****
iBody **3**	71,200	aspartic proteases	31,000 ± 23*****
Compound **4**	1,159	His-tag sequence	ND
iBody **4**	109,000	His-tag sequence	ND
iBody **5**	96,100	negative control	ND
iBody **6**	59,500	negative control	ND

***** K_i values were determined for wild-type HIV-1 protease.

& Šácha *et al.*, manuscript in preparation

5.2. Inhibition of HIV-1 protease by low molecular weight HIV-1 protease inhibitors and iBodies

Inhibition of HIV-1 protease was determined using hydrolysis of a chromogenic peptide substrate. When the peptide is cleaved, the absorbance at 305 nm decreases, and cleavage rate is monitored by UV spectroscopy. For determination of inhibition constants (IC_{50} and K_i), v_i/v_0 ratio was used (**Fig. 11, p. 38**). Obtained inhibition constants are summarized in the **Table 3.** For experimental details see Methods (**p. 22).**

Table 3: Obtained inhibition constants of HIV-1 protease inhibitors and iBodies towards HIV-1 protease.

	IC_{50} [nM]	**K_i [nM]**
Compound 2	0.0380 ± 0.007	0.0120 ± 0.0001
iBody 2	12.7 ± 1.3	7.3 ± 0.5
Compound 3	852 ± 63	602 ± 2
iBody 3	65.4 ± 2.5	31.0 ± 0.2

Compound 2 is a derivative of ritonavir, an FDA approved HIV PR inhibitor, with a linker enabling its covalent attachment to a polymer carrier (see **Fig. 10, p. 34**). The K_i value of Compound 2 was determined to 12 ± 0.1 pM, while the iBody 2 possessed K_i value of 7.3 ± 0.5 nM. Thus, the conjugation of Compound 2 with HPMA copolymer resulted in approx. 600-fold increase of the K_i value.

Compound 3 is a derivative of pepstatin, a class-specific inhibitor of aspartic proteases, again modified with a linker to enable covalent attachment of the compound to the HPMA backbone (see **Fig. 10, p. 34**). The K_i value of Compound 3 was determined to 602 ± 2 nM and its conjugation with HPMA copolymer (yielding iBody 3), resulted in 20-fold decrease of the K_i value (31.0 ± 0.2 nM), which was in agreement with our assumption.

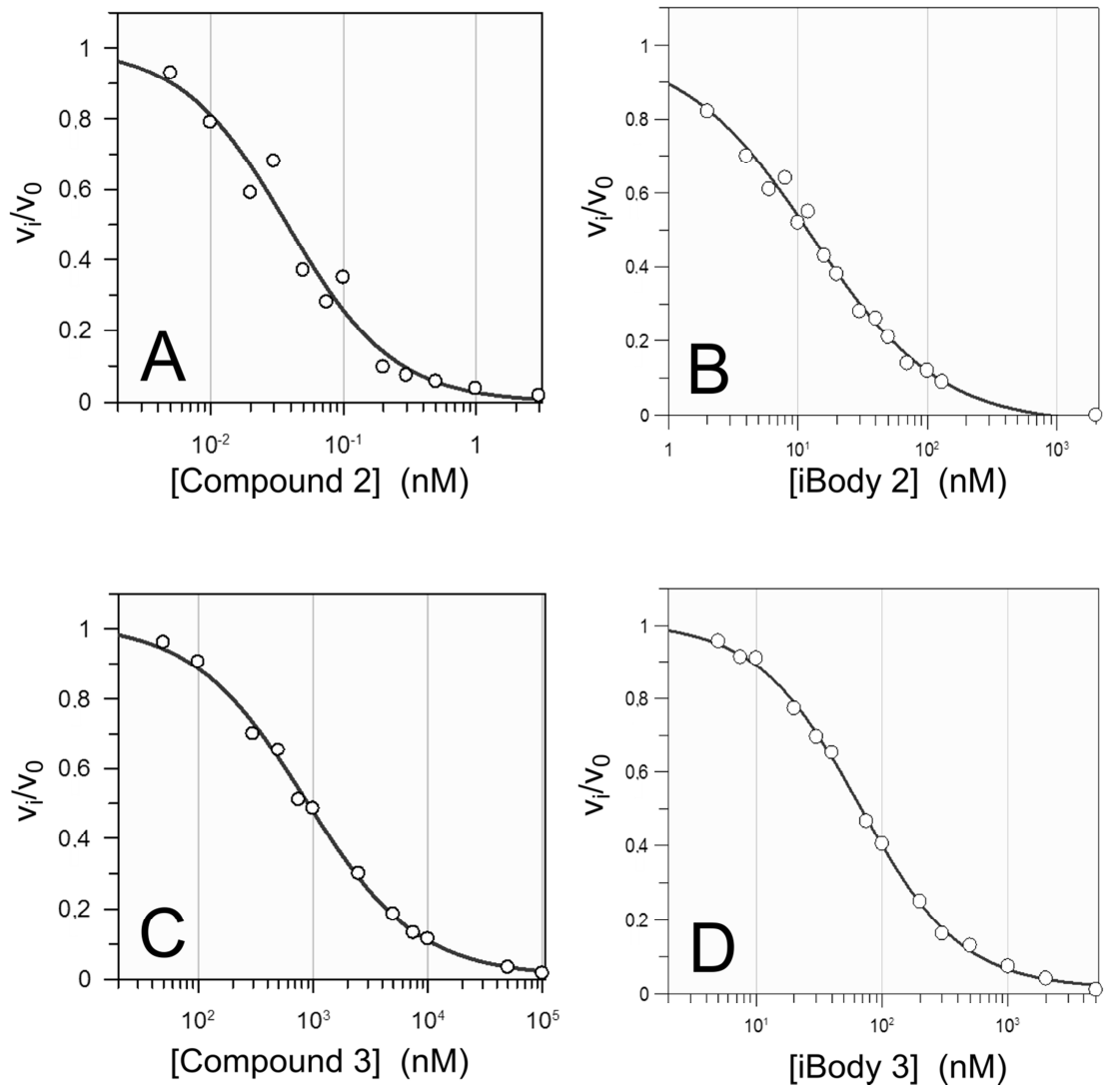

Figure 11: Inhibition of HIV-1 protease. The substrate KARVNle*NphEANle-NH_2 was cleaved by recombinant purified HIV-1 protease in the presence of various concentrations of inhibitors as described in the Methods (**p. 22**). The non-linear data fits for the determination of IC_{50} (Panels A, B, C, and D) and K_i values were carried out in program Grafit 7.0.2. Panel A: Compound 2. Panel B: iBody 2. Panel C: Compound 3. Panel D: iBody 3. Obtained inhibition constants are summarized in **Table 3, p. 37**.

5.3. Inhibition of pepsin with iBody 3

iBody 3 (Fig 1) is a HPMA copolymer that contains compound 3, a modified pepstatin, as a targeting group. We set to analyze the inhibitory activity of this compound to its cognate enzyme, pepsin. For determination of the inhibition constants of iBody 3 for pepsin, the fluorimetric assay was used. The pepsin substrate (Abz-Lys-Pro-Ala-Glu-Phe-Nph-Ala-Leu) contains an Abz group used for FRET application. The product of hydrolysis was continuously monitored by an increase of fluorescence. For experimental details see Methods (**p. 23)**.

K_m value of pepsin for the substrate was determined as 12.5 µM and k_{cat} value as 43.4 s^{-1}. The ratio k_{cat}/K_m was then equal to $3.51 \cdot 10^6$ $M^{-1}s^{-1}$. The inhibition constants were determined from the dose-response plot. The ratios v_i/v_0, measured for a set of concentrations, were plotted and fitted in program Grafit 7.0.2 (**Fig. 12**). For iBody 3, IC_{50} was determined as 2.25 ± 0.24 nM and K_i as 0.0294 ± 0.022 nM. iBody 3 inhibited pepsin almost four times better than the original acetyl-pepstatin did.

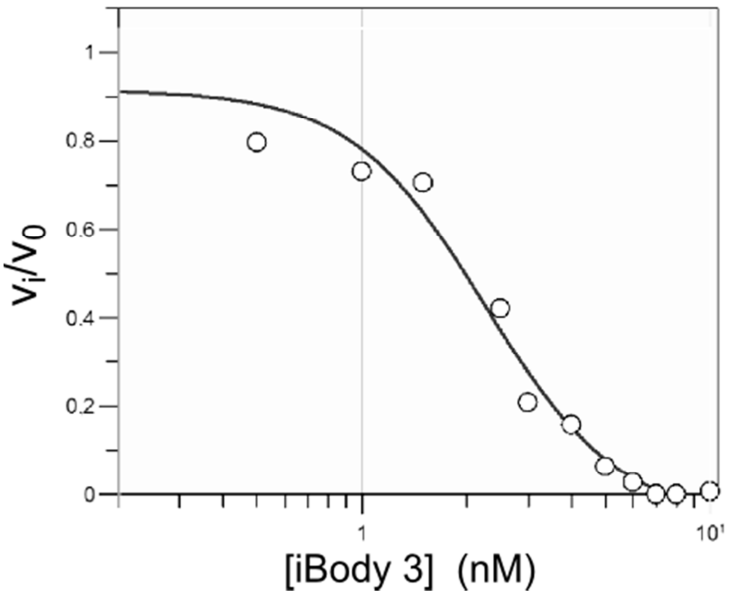

Figure 12: Inhibition of pepsin with iBody 3. The substrate Abz-Lys-Pro-Ala-Glu-Phe-Nph-Ala-Leu was cleaved by pepsin in the presence of various concentrations of iBody 3 as described in the Methods (**p. 23**). Obtained inhibition constants are summarized in **Table 3, p. 37**. The non-linear data fit for the determination of IC_{50} (this figure) and K_i values was performed in Grafit 7.0.2.

5.4. Quantification of iBody 1 binding to GCPII by surface plasmon resonance (SPR)

Using surface plasmon resonance, we analyzed association and dissociation kinetics of iBody 1 binding to GCPII. First, monoclonal antibody against GCPII (D2B [70]) was immobilized to a gold SPR chip. Subsequently, Avi-GCPII [71] was bound to D2B antibody and finally, iBody 1 in four different concentrations was loaded on the chip (association, k_{on}). Afterwards, the buffer only was loaded (dissociation, k_{off}). For experimental details see Methods (**p. 24)**. Data from the SPR measurement were fitted and interaction constants were calculated using program TraceDrawer 1.5 (**Fig. 13)**. Since the obtained dissociation phase constant k_{off} was under the detection limit of the used SPR machine, the K_D value could not be determined precisely (K_D is lower than 64 pM).

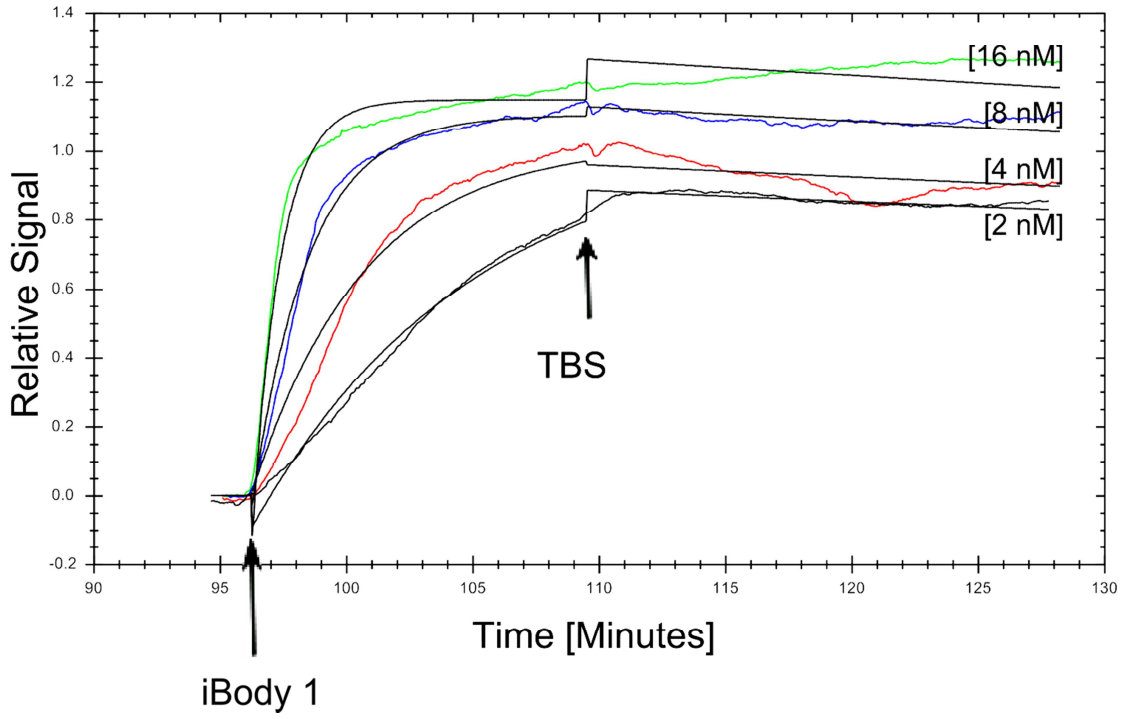

Figure 13: Interaction of GCPII with iBody 1. To determine K_D of iBody 1, four concentrations (2, 4, 8, and 16 nM) were loaded onto immobilized Avi-GCPII. For experimental details see Methods (**p. 24)**. After measuring the association and dissociation curves, data were fitted and K_D was determined using program TraceDrawer 1.5.

5.5. Affinity purification of GCPII from LNCaP lysate

In this experiment, iBody 1 was tested for its ability to isolate GCPII from cell lysate, iBody 5 (HPMA copolymer without GCPII-inhibitor, see Fig. **10**) was used as a negative control. GCPII-specific monoclonal antibody (J591, kindly provided by N.H. Bander, Cornell University, New York) bound to Protein G Sepharose served as positive control, blank Protein G Sepharose resin served as negative control for J591 reaction. First, iBodies were prebound to Streptavidin Agarose resin and the samples were incubated with a cell lysate containing GCPII (LNCaP cells were used), then the resin was washed and bound proteins were eluted using reducing SDS-PAGE sample buffer. Afterwards, the samples were resolved using SDS-PAGE, proteins blotted onto a nitrocellulose membrane and immunostained using a GCPII-specific antibody (GCP-04 [70]) (**Fig. 14**). For experimental details see Methods (**p. 25)**. iBody 1 showed equal ability to isolate GCPII from the lysate as antibody J591. iBody 5 and blank resin, which served as negative controls, bound a marginal amount of GCPII.

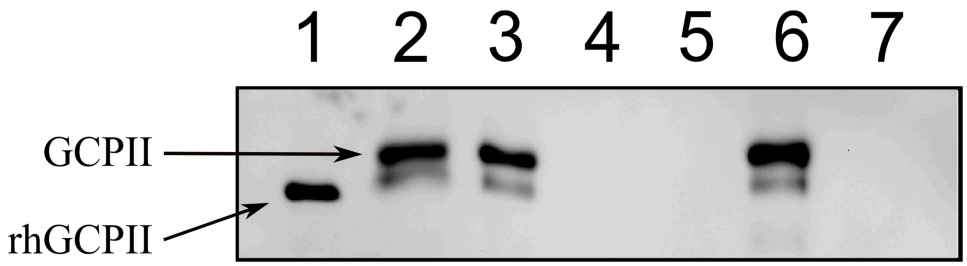

Figure 14: The Western blot analysis of GCPII affinity purification from LNCaP lysate. Lane 1: 5 ng of recombinant human extracellular GCPII (aminoacids 44-750, rhGCPII, [42]). Lane 2: LNCaP cell lysate. Lane 3: iBody 1 elution. Lane 4: iBody 5 elution. Lane 5: blank Streptavidin Agarose resin elution. Lane 6: GCPII-specific monoclonal antibody (J591) elution. Lane 7: blank Protein G Sepharose resin elution. Five microliters of sample was loaded into each lane. For experimental details see Methods (**p. 25**).

5.6. Affinity purification of HIV-1 protease from cell lysate

In this experiment, iBodies 2 and 3 were tested for their ability to isolate HIV-1 protease from LNCaP lysate spiked by recombinant HIV protease. iBody 6 served as a negative control. Samples were incubated with LNCaP lysate spiked with HIV-1 protease, washed and eluted with reducing sample buffer. Afterwards, the samples were resolved by SDS-PAGE and proteins were visualized with silver-staining (**Fig. 15**). iBody 2 and iBody 3 possess the ability to isolate HIV-1 protease from cell lysate, whereas iBody 6, lacking the targeting ligand, isolated only a small amount of the protein.

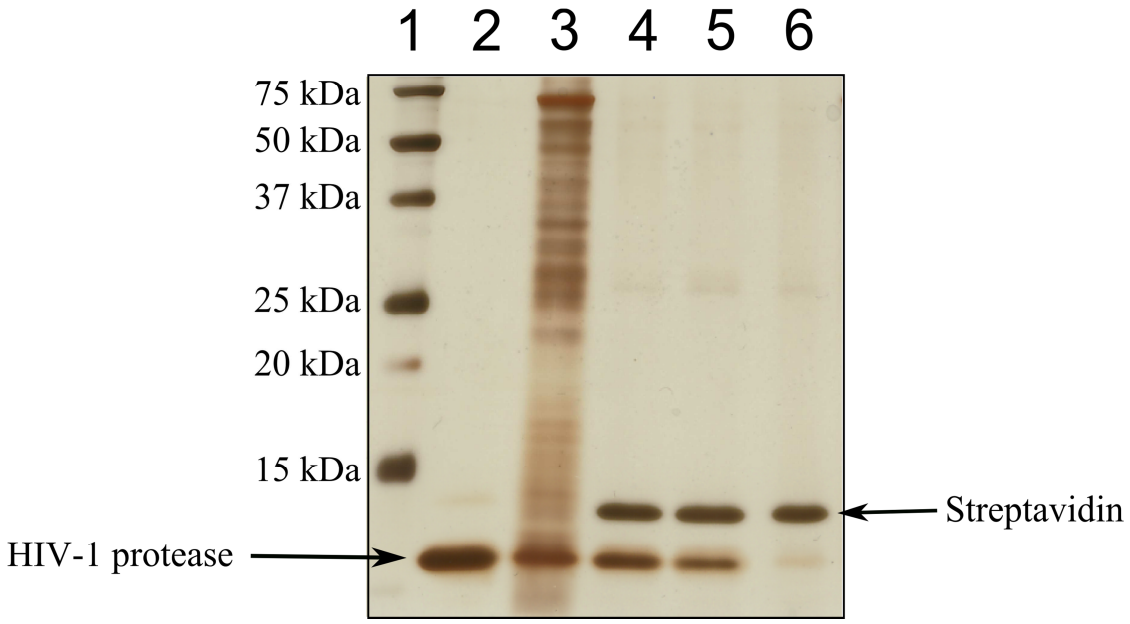

Figure 15: The SDS-PAGE analysis of HIV-1 protease affinity purification from the spiked LNCaP lysate. Lane 1: All Blue Standards (1 µl). Lane 2: HIV-1 protease standard (600 ng). Lane 3: LNCaP lysate spiked with HIV-1 protease. Lane 4: iBody 2 elution. Lane 5: iBody 3 elution. Lane 6: iBody 6 elution. Ten microliters was loaded into each lane. Streptavidin, present in lanes 4-6, was released from Streptavidin Agarose during the elution step. For experimental detail see Methods (**p. 26**).

5.7. Affinity purification of pepsin from cell lysate

In this experiment, the iBody 3 was tested for its ability to bind pepsin, another representative of aspartic proteases. iBody 6 (a HPMA copolymer identical to iBody 3 without the targeting pepstatin derivative) served as a negative control. Samples were incubated with pepsin-spiked LNCaP lysate, washed and eluted with reducing sample buffer. Afterwards, the samples were resolved by SDS-PAGE and proteins were visualized by silver-staining (**Fig. 16**). iBody 3 presented the ability to isolate pepsin from the cell lysate, whereas iBody 6 with no targeting ligand did not isolate the target protein.

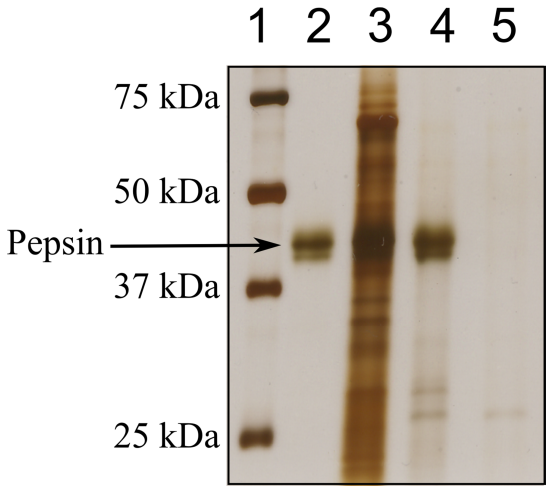

Figure 16: The SDS-PAGE analysis of pepsin affinity purification from spiked LNCaP lysate. Lane 1: All Blue Standards (1 µl). Lane 2: Pepsin standard (2 µg). Lane 3: LNCaP lysate spiked with pepsin Lane 4: iBody 3 elution. Lane 5: iBody 6 elution. Five microliters was loaded into each lane. For experimental details see Methods (**p. 26**).

5.8. Affinity purification of Ddi1-HisTag from *E. coli* lysate

To prove the ability of our iBodies to specifically bind His-tagged proteins, Ddi1-HisTag was isolated from *E. coli* lysate using iBody 4 (HPMA copolymer containing nitrilotriacetic acid derivative capable of binding the hexahistidine sequence (see **Fig. 10, p. 34**). As a negative control was used iBody 5 lacking any targeting group. Another negative control was blank resin Streptavidin Agarose. iBodies were bound to Streptavidin Agarose resin and then they were incubated with *E. coli* lysate. After incubation, resin was washed and bound proteins were eluted with 1 M imidazole. Samples were resolved by SDS-PAGE, and proteins were visualized by silver-staining procedure (**Fig. 17**). iBody 4 was able to isolate Ddi1-HisTag, whereas iBody 5 without any targeting ligand, did not bind any Ddi1-HisTag (a band of the same intensity was present in both iBody 5 and blank Streptavidin Agarose resin lanes suggesting non-specific binding was caused by the resin, not by the iBody itself).

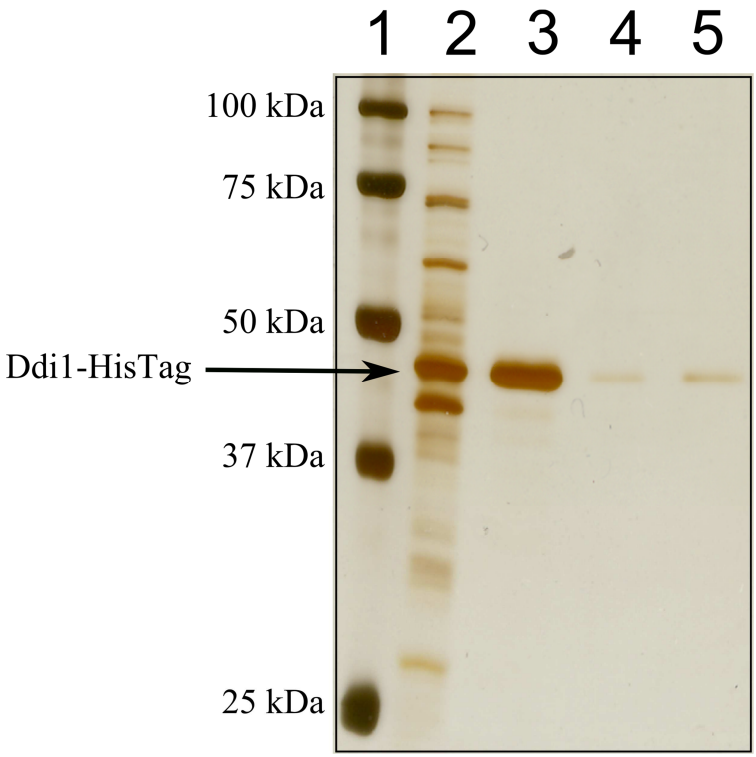

Figure 17: The SDS-PAGE analysis of Ddi1-HisTag affinity purification from *E. coli* lysate. Lane 1: All Blue Standards (1 μl). Lane 2: *E. coli* lysate. Lane 3: iBody 4 elution. Lane 4: iBody 5 elution. Lane 5: blank resin elution. Fifteen microliters was loaded into each lane. For experimental details see Methods (**p. 27**).

5.9. Application of iBodies for immunochemistry: *Flow cytometry*

To find out if iBody 1 can specifically bind GCPII on the membrane of LNCaP cells (endogenously expressing GPCII), flow cytometry experiment was performed. As a positive control, fluorescently labeled monoclonal antibody against GCPII (2G7-ATTO 488) [70] was used. As negative controls, iBody 5 (lacking the inhibitor of GCPII) and PC3 cells (not expressing GCPII) were used. Cells were incubated with iBodies or 2G7-ATTO 488, washed with PBS, and then analyzed using flow cytometry (**Fig. 18, p. 46**). iBody 1 stained GCPII positive cells as well as the fluorescent antibody conjugate 2G7-ATTO 488. GCPII-negative cells PC3 did bind neither iBody 1, nor iBody 5, however, they were slightly stained by 2G7-ATTO488 conjugate. Therefore, iBody-based staining seems to suffer from smaller non-specific binding produced by the fluorescent conjugate.

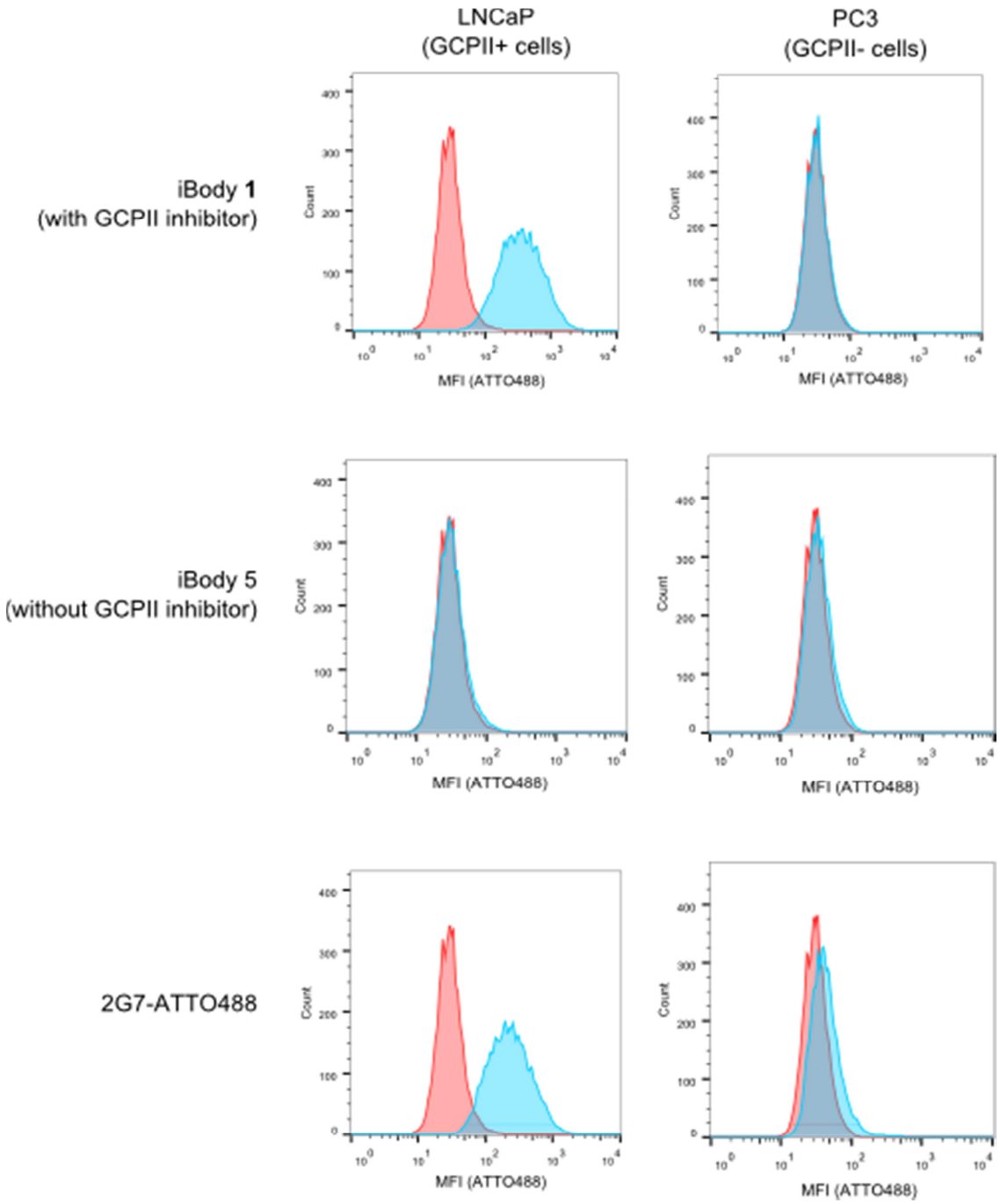

Figure 18: Analysis of LNCaP and PC3 cells stained with iBodies by flow cytometry. LNCaP cells (GCPII+) and PC3 cells (GCPII-) were incubated with iBody 1, iBody 5 and GCPII-specific monoclonal antibody conjugated with a fluorescent dye (2G7-ATTO 488). Cells treated with iBodies or antibody are depicted in red, whereas the population of untreated cells is shown in blue. Experimental details are given in Methods (**p. 31**).

5.10. Application of iBodies for immunochemistry: *Cell imaging by confocal microscopy*

The aim of this experiment was to compare fluorescent labeling of LNCaP cells (expressing GPCII) with iBody 1 and fluorescently labeled monoclonal antibody against GCPII (2G7-ATTO 488). To verify specificity of binding, PC3 cells not expressing GCPII were used. As another negative control, iBody 5, lacking the GCPII inhibitor, was used as well. Cells were incubated with iBodies or 2G7-ATTO 488, then washed, fixed and analyzed with a confocal microscope (**Fig. 19, p. 48**). iBody 1 stained GCPII positive cells even better than the fluorescent antibody 2G7-ATTO 488 did. The iBodies did not suffer from any non-specific binding and only minimal nonspecific signal of 2G7-ATTO 488 was observed, which is in an agreement with flow cytometry experiment.

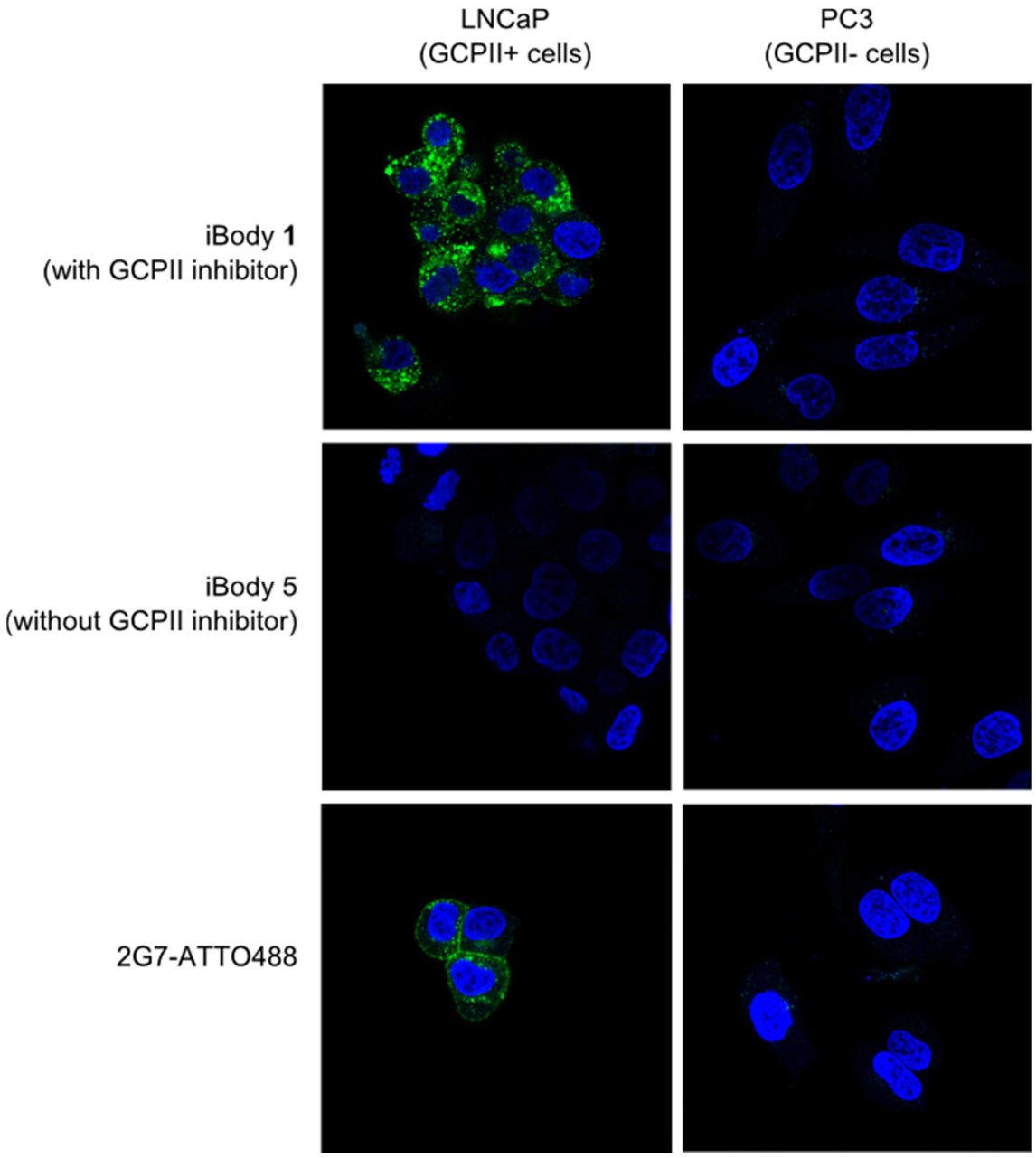

Figure 19: Analysis of LNCaP and PC3 cells by confocal microscopy. LNCaP cells (GCPII+) and PC3 cells (GCPII-) were incubated with iBody 1, iBody 5 and GCPII-specific monoclonal antibody (conjugated with fluorescent dye; 2G7-ATTO 488) and stained by Hoechst 34580. Cell nuclei are depicted in blue, ATTO 488 provides green fluorescence. Experimental details are given in Methods (**p. 32**).

6. Discussion

As described in the first chapter, *N*-(2-hydroxypropyl)methacrylamide (HPMA) copolymers attract interest of medicinal chemists for number of reasons. First of all, HPMA polymers are very well tolerated *in vivo*. High biocompatibility allowed these hydrophilic macromolecules to be used as synthetic drug carriers. Second, synthesis of HPMA copolymers was well described and it is possible to synthesize these macromolecules according to elaborate protocols. Third, the polymer backbone of HPMA copolymers is very stable and it undergoes very slow biodegradation *in vivo*. Furthermore, the copolymers are highly modular: *e.g.*, a linker connecting the drug to the backbone can be prepared either as non-cleavable or cleavable under particular conditions (for example, in endosomes after internalization).

In the past, HPMA copolymers developed as anticancer agents were targeted to tumor tissue only by the EPR effect (due to defected lymphatic drainage and subsequent accumulation of macromolecules in the solid tumors). Our approach is more specific: we prepared HPMA copolymers with a targeting group, namely, with inhibitors of selected therapeutically important proteins (GCPII, HIV-1 protease or pepsin). Furthermore, targeted protein does not have to be a protein with enzymatic activity; it can be any protein with a known ligand (e.g., a His-tagged protein). Apart from a targeting group, the HPMA copolymers developed in Jan Konvalinka group possess also an affinity anchor (such as biotin), and a reporter group (typically a fluorophore). For our purpose, biotin was chosen as the affinity anchor, and as the reporter group, a fluorescent dye ATTO 488 was selected. This fluorescent dye was specially designed for life sciences: it is very hydrophilic and excited by ion-argon laser. Biotin was selected because it can be quickly and very firmly immobilized to a number of commercially available resins (*e.g.* Streptavidin Agarose).

Due to their specific properties towards the targeted proteins, our HPMA copolymers were denominated **iBodies**. This name is a conjunction of words “inhibitor” and “antibodies”. This name also reflects the fact that iBodies might serve as a fully synthetic substitution of antibodies in a number of immunochemistry methods in addition to being an interesting drug delivery vehicle. However, there is a significant difference between antibodies and iBodies: antibodies usually recognize an amino acid sequence located on a protein surface, while

iBodies target a protein function. In other words, the function of iBody (containing an enzyme inhibitor) demands a functional enzyme in its native state.

An advantage of iBodies is also their fully synthetic character. Due to their fully synthetic nature, iBodies are, compared with antibodies, very cheap bioactive agents. Rough estimation is that iBodies can be as much as thousand-times cheaper than antibodies. Whereas shelf-life of antibodies is limited, iBodies are, again due to their synthetic nature, stable macromolecules without any tendency to degradation.

To show that iBodies could functionaly replace antibodies in various immunochemical assays; they were used for affinity purification, confocal microscopy, and flow cytometry. Moreover, iBodies were also successfully used in ELISA, wherein they replaced commonly used antibodies (Šácha *et al*., manuscript in preparation).

So far, iBodies have been tested only on a few proteins. In future, we would like to expand our iBodies repertoire to target more protein. Nowadays, our laboratory is already testing iBodies that target other clinically relevant proteins, such as carbonic anhydrase IX and neuraminidase.

Characterization of inhibition effects was determined using a different method for each enzyme. For GCPII, inhibition effect was calculated from SPR-obtained association and dissociation curves. In the case of HIV-1 protease, inhibition assay was performed according to the previously published protocol based on the hydrolysis of chromogenic substrate [66]. Pepsin inhibition was determined using a fluorogenic peptide substrate, which was originally designed for cathepsin D enzymatic activity assay [69].

The interaction profile of iBody 1 to GCPII was determined using SPR analysis. SPR is a robust and quick method for K_D determination. K_D value of this interaction is lower than 64 pM, which makes iBody 1 comparable with the best monoclonal antibodies against GCPII [70].

Compound 2, which is a derivate of ritonavir, presented a strong inhibiting effect to HIV-1 protease (K_i of 12 ± 0.1 pM). Ritonavir exhibits $K_i = 15 \pm 2$ pM towards HIV-1 protease [77]. iBody 2, which is a macromolecular conjugate of Compound 2, showed a significant increase of the K_i value ($K_i = 7.34 \pm 0.46$ nM). In spite of this decrease in inhibition effect, iBody was shown to be suitable for affinity purification of HIV-1 protease from cell lysate. We speculate that the decrease of inhibition effect after conjugation can be caused by a sterical hindrance of inhibitor on the polymer backbone.

A pepstatin derivate, Compound 3, showed a good inhibiting effect to HIV-1 protease (K_i of 602 ± 1.7 nM). K_i for acetyl-pepstatin was previously determined as 116 ± 5 nM [77]. iBody 3 showed approximately twenty times better inhibition effect (K_i of 31 ± 0.22 nM) than the maternal Compound 3. Compared to the situation with Compound 2 and iBody 2, the situation of Compound 3 and iBody 3 is different. In this case, the conjugation of Compound 2 to the polymer backbone led to macromolecule with better inhibition properties.

Inhibitors which we chose for the synthesis of presented iBodies, are tight binding ligands of the targeted enzymes. Unfortunately, due to this fact, the tested iBodies are not suitable for the protein purification. The best application for the iBodies would be then the native protein isolation/detection. In addition, it is possible to design iBodies with weaker inhibitors of targeted proteins, which would serve well to the protein purification.

Because of the tight binding, the iBodies discussed above and bind their target proteins so tightly that the elution of the proteins can be done only under harsh conditions (98 °C for 10 minutes). However, in the case of anti-His-tag iBody, it was possible reversibly bind protein with His-tag (Ddi1-HisTag), which could be eluted using 1 M imidazole solution. This iBody contains a tris-(nitrilotriacetic) acid group which has 10 nM affinity to the hexahistidine sequence (NTA group has affinity of 10 μM) [78]. This approach is an analogy to the Ni-NTA protein purification system. Furthermore, the anti-His-tag iBody was successfully used for His-tagged protein detection on Western blot, with better sensitivity than anti-hexahistidine antibody used (Šácha *et al.*, manuscript in preparation). The above mentioned iBodies containing enzyme inhibitors cannot be used on Western blots, since they bind only an intact active site of the native enzyme.

GCPII was successfully isolated from LNCaP cell lysate using specific iBody decorated by a GCPII inhibitor (iBody 1). The amount of GCPII isolated with iBody 1 is comparable with that isolated using the anti-GCPII antibody J591. Furthermore, in the negative control elutions (iBody 5 lacking the GCPII inhibitor and blank resin), there was no GCPII, which confirms the high specificity of iBody 1.

iBody 2, which contains a ritonavir derivate (Compound 2), a potent inhibitor of HIV-1 protease, showed potential to isolate HIV-1 protease from the mammalian cell lysate. Rough estimation from electrophoretogram is that iBody 2 (containing ritonavir derivative) has a better affinity to HIV-protease than iBody 3 (contaning pepstatin derivative). This visual estimation was confirmed by inhibition measurements, which determined the K_i value of iBody 2 as four times lower than K_i value of iBody 3.

To prove that iBody 3 binds aspartate proteases, HIV-1 protease and pepsin were chosen as the model proteins. Using an iBody 6 as negative control in both reactions, the high specificity and good protein yields were obtained in the elution fractions of iBody 3.

LNCaP (GCPII positive) and PC3 (GCPII negative) cells were used for fluorescent visualization of GCPII on cell membrane. Cells were incubated with iBody 1 (with GCPII inhibitor), iBody 5 (without GCPII inhibitor) and 2G7-ATTO 488 (monoclonal antibody against GCPII conjugated with fluorescent group ATTO 488). The result of confocal microscopy and flow cytometry is promising - GCPII was detected only in LNCaP cells incubated with iBody 1 and 2G7-ATTO 488. The fluorescence signal in the control cells not expressing GCPII was negligible which means that specificity of these assays is very good. In terms of fluorescent imaging using confocal fluorescent microscopy, iBody 1 labeled GCPII-expressing mammalian cells LNCaP even better than the fluorescently labeled antibody 2G7-ATTO 488 did.

7. Conclusions

- iBodies, HPMA copolymers decorated by low molecular weight targeting ligand, fluorophore (ATTO 488) and an affinity anchor (biotin) have been recently developed in Konvalinka laboratory
- The ability of specific iBodies to inhibit corresponding cognate enzymes (aspartic protease pepsin, HIV protease and glutamate carboxypeptidase II) was evaluated using enzymatic assays
- The specificity of binding of iBodies was evaluated by their ability to bind and separate the target protein from cell lysate specifically
- iBodies decorated by specific glutamate carboxypeptidase II inhibitors and a fluorophore were used for specific imaging of GCPII-expressing mammalian cells and their analysis by flow cytometry
- iBody with GCPII-inhibitor labeled GCPII positive cells with better efficiency than the specific monoclonal antibody did
- HPMA copolymers decorated by analogs of nitrilotriacetic acid were used to visualize His-tagged proteins in complex mixtures by Western blotting
- Tested iBodies were shown to represent an interesting synthetic replacement for monoclonal antibodies in a number for immunochemistry applications.

8. List of Abbreviations

2G7	Monoclonal antibody against GCPII
7E11-C5.3	Monoclonal antibody against GCPII
Abz	Aminobenzoic acid
APS	Ammonium persulfate
Asp_8	Octapeptide of D-aspartic acids
BSA	Bovine serum albumin
CCD	Charge-coupled device
D2B	Monoclonal antibody against GCPII
Da	Dalton
Ddi	DNA damage-inducible protein
DMEM	Dulbecco's Modified Eagle's medium
DMSO	Dimethyl sulphoxide
EDTA	Ethylendiaminetetraacetic acid
EPR	Enhanced permeability and retention
FRET	Fluorescence resonance energy transfer
GCPII	Glutamate Carboxypeptidase II
HEPES	4-(2-hydroxyethyl)-1-piperazineethanesulfonic acid
HPMA	*N*-(2-hydroxypropyl)methacrylamide
LNCaP	Lymph node carcinoma of the prostate (cell line expressing GCPII))
MRI	Magnetic resonance imaging
NAAG	*N*-acetyl-L-aspartyl-L-glutamate
Nph	4-nitrophenylalanine
PAGE	polyacrylamide gel electrophoresis
PBS	Phosphate buffered saline

PBST	Phosphate buffered saline containing 0.1 % Tween
PC3	Prostate cancer cell line (not expressing GCPII)
PDB	Protein data bank
PGE_1	Prostaglandin E_1
PSMA	Prostate-specific membrane antigen
rhGCPII	Recombinant human extracellular GCPII;
	(Extracellular part of human GCPII with aminoacids 44-750)
RPMI	Roswell Park Medical Institute medium
SDS	Sodium dodecyl sulphate
SDS-PAGE	Sodium dodecyl sulphate polyacrylamide gel electrophoresis
SPR	Surface Plasmon Resonance
TEMED	*N*,*N*,*N*',*N*'- tetramethylethylenediamine
Tris	Tris(hydroxymethyl)aminomethane
tris-NTA	Tris-(nitrilotriacetic acid)
TBS	Tris buffered saline

9. References

1. Duncan R., Kopeček J., Soluble synthetic polymers as potential drug carriers, in: Polymers in Medicine, vol. 57, Springer Berlin Heidelberg, 1984, 51-101.

2. Kopecek J., Kopeckova P.: HPMA copolymers: origins, early developments, present, and future. Adv Drug Deliv, 62 (2010) 122-149.

3. Ulbrich K., Subr V.: Structural and chemical aspects of HPMA copolymers as drug carriers. Adv Drug Deliv, 62 (2010) 150-166.

4. Kopecek J., Ulbrich K., Vacik J., Strohalm J., Chytry V., Drobnik J., Kalal J., Copolymers based on N-substituted acrylamides, N-substituted methacrylamides and N,N-disubstituted acrylamides and the method of their manufacturing, Patent, 1977.

5. Drobnik J., Kopecek J., Labsky J., Rejmanova P., Exner J., Kalal J., Amino acid, acrylate or acrylamide addition polymer, Patent, 1978.

6. Kopecek J., Rejmanova P., Strohalm J., Ulbrich K., Rihova B., Chytry V., Lloyd J. B., Duncan R., Hydroxypropylmethacrylamide polymer with peptide side chains to which are attached drugs for delivery to target cells, Patent, 1991.

7. Rihova B., Kopeckova P., Strohalm J., Rossmann P., Vetvicka V., Kopecek J.: Antibody-directed affinity therapy applied to the immune system: in vivo effectiveness and limited toxicity of daunomycin conjugated to HPMA copolymers and targeting antibody. Clin Immunol Immunopathol, 46 (1988) 100-114.

8. Rihova B., Kopecek J., Kopeckova-Rejmanova P., Strohalm J., Plocova D., Semoradova H.: Bioaffinity therapy with antibodies and drugs bound to soluble synthetic polymers. J Chromatogr, 376 (1986) 221-233.

9. Kopecek J.: Polymer-drug conjugates: origins, progress to date and future directions. Adv Drug Deliv, 65 (2013) 49-59.

10. Minko T., Kopeckova P., Kopecek J.: Chronic exposure to HPMA copolymer-bound adriamycin does not induce multidrug resistance in a human ovarian carcinoma cell line. J Control Release, 59 (1999) 133-148.

11. Bertrand N., Leroux J. C.: The journey of a drug-carrier in the body: an anatomo-physiological perspective. J Control Release, 161 (2012) 152-163.

12. Matsumura Y., Maeda H.: A new concept for macromolecular therapeutics in cancer chemotherapy: mechanism of tumoritropic accumulation of proteins and the antitumor agent smancs. Canc Res, 46 (1986) 6387-6392.

13. Maeda H., Wu J., Sawa T., Matsumura Y., Hori K.: Tumor vascular permeability and the EPR effect in macromolecular therapeutics: a review. J Control Release, 65 (2000) 271-284.

14. Maeda H., Matsumoto T., Konno T., Iwai K., Ueda M.: Tailor-making of protein drugs by polymer conjugation for tumor targeting: A brief review on smancs. J Protein Chem, 3 (1984) 181-193.

15. Vasey P. A., Kaye S. B., Morrison R., Twelves C., Wilson P., Duncan R., Thomson A. H., Murray L. S., Hilditch T. E., Murray T., Burtles S., Fraier D., Frigerio E., Cassidy J.: Phase I clinical and pharmacokinetic study of PK1 [N-(2-hydroxypropyl)methacrylamide copolymer doxorubicin]: first member of a new class of chemotherapeutic agents-drug-polymer conjugates. Cancer Research Campaign Phase I/II Committee. Clin Cancer Res, 5 (1999) 83-94.

16. Tacar O., Sriamornsak P., Dass C. R.: Doxorubicin: an update on anticancer molecular action, toxicity and novel drug delivery systems. J Pharm Pharmacol, 65 (2013) 157-170.

17. Seymour L. W., Ferry D. R., Kerr D. J., Rea D., Whitlock M., Poyner R., Boivin C., Hesslewood S., Twelves C., Blackie R., Schatzlein A., Jodrell D., Bissett D., Calvert H., Lind M., Robbins A., Burtles S., Duncan R., Cassidy J.: Phase II studies of polymer-doxorubicin (PK1, FCE28068) in the treatment of breast, lung and colorectal cancer. Int J Oncol, 34 (2009) 1629-1636.

18. Gianasi E., Wasil M., Evagorou E. G., Keddle A., Wilson G., Duncan R.: HPMA copolymer platinates as novel antitumour agents: in vitro properties, pharmacokinetics and antitumour activity in vivo. Eur J Cancer, 35 (1999) 994-1002.

19. Bouma M., Nuijen B., Stewart D. R., Shannon K. F., St John J. V., Rice J. R., Harms R., Jansen B. A., van Zutphen S., Reedijk J., Bult A., Beijnen J. H.: Pharmaceutical quality control of the investigational polymer-conjugated platinum anticancer agent AP 5280. PDA J Pharm Sci Technol, 57 (2003) 198-207.

20. Lin X., Zhang Q., Rice J. R., Stewart D. R., Nowotnik D. P., Howell S. B.: Improved targeting of platinum chemotherapeutics. the antitumour activity of the HPMA copolymer platinum agent AP5280 in murine tumour models. Eur J Cancer, 40 (2004) 291-297.

21. Rademaker-Lakhai J. M., Terret C., Howell S. B., Baud C. M., De Boer R. F., Pluim D., Beijnen J. H., Schellens J. H., Droz J. P.: A Phase I and pharmacological study of the platinum polymer AP5280 given as an intravenous infusion once every 3 weeks in patients with solid tumors. Clin Cancer Res, 10 (2004) 3386-3395.

22. Satchi-Fainaro R., Puder M., Davies J. W., Tran H. T., Sampson D. A., Greene A. K., Corfas G., Folkman J.: Targeting angiogenesis with a conjugate of HPMA copolymer and TNP-470. Nat Med, 10 (2004) 255-261.

23. Vicent M. J.: Polymer-drug conjugates as modulators of cellular apoptosis. AAPS J, 9 (2007) E200-207.

24. Oman M., Liu J., Chen J., Durrant D., Yang H.-S., He Y., Kopeckova P., Kopecek J., Lee R.-M.: Using N-(2-hydroxypropyl)methacrylamide copolymer drug bioconjugate as a novel approach to deliver a Bcl-2-targeting compound HA14-1 in vivo. AACR Meeting Abstract, (2005) 333-338.

25. Meerum Terwogt J. M., ten Bokkel Huinink W. W., Schellens J. H., Schot M., Mandjes I. A., Zurlo M. G., Rocchetti M., Rosing H., Koopman F. J., Beijnen J. H.: Phase I clinical and pharmacokinetic study of PNU166945, a novel water-soluble polymer-conjugated prodrug of paclitaxel. Anticancer Drugs, 12 (2001) 315-323.

26. Schoemaker N. E., van Kesteren C., Rosing H., Jansen S., Swart M., Lieverst J., Fraier D., Breda M., Pellizzoni C., Spinelli R., Grazia Porro M., Beijnen J. H., Schellens J. H., ten Bokkel Huinink W. W.: A phase I and pharmacokinetic study of MAG-CPT, a water-soluble polymer conjugate of camptothecin. Br J Cancer, 87 (2002) 608-614.

27. Bissett D., Cassidy J., de Bono J. S., Muirhead F., Main M., Robson L., Fraier D., Magne M. L., Pellizzoni C., Porro M. G., Spinelli R., Speed W., Twelves C.: Phase I and pharmacokinetic (PK) study of MAG-CPT (PNU 166148): a polymeric derivative of camptothecin (CPT). Br J Cancer, 91 (2004) 50-55.

28. Pan H., Kopeckova P., Wang D., Yang J., Miller S., Kopecek J.: Water-soluble HPMA copolymer--prostaglandin E1 conjugates containing a cathepsin K sensitive spacer. J Drug Target, 14 (2006) 425-435.

29. Liu X. M., Miller S. C., Wang D.: Beyond oncology--application of HPMA copolymers in non-cancerous diseases. Adv Drug Deliv, 62 (2010) 258-271.

30. Miller S. C., Pan H., Wang D., Bowman B. M., Kopeckova P., Kopecek J.: Feasibility of using a bone-targeted, macromolecular delivery system coupled with prostaglandin E(1) to promote bone formation in aged, estrogen-deficient rats. Pharm Res, 25 (2008) 2889-2895.

31. Pan H., Sima M., Miller S. C., Kopeckova P., Yang J., Kopecek J.: Efficiency of high molecular weight backbone degradable HPMA copolymer-prostaglandin E1 conjugate in promotion of bone formation in ovariectomized rats. Biomaterials, 34 (2013) 6528-6538.

32. Wang D., Miller S. C., Shlyakhtenko L. S., Portillo A. M., Liu X. M., Papangkorn K., Kopeckova P., Lyubchenko Y., Higuchi W. I., Kopecek J.: Osteotropic Peptide that differentiates functional domains of the skeleton. Bioconjug Chem, 18 (2007) 1375-1378.

33. Wang D., Miller S. C., Sima M., Parker D., Buswell H., Goodrich K. C., Kopeckova P., Kopecek J.: The arthrotropism of macromolecules in adjuvant-induced arthritis rat model: a preliminary study. Pharm Res, 21 (2004) 1741-1749.

34. Bendele A.: Animal models of rheumatoid arthritis. J Musculoskelet Neuronal Interact, 1 (2001) 377-385.

35. Quan L. D., Purdue P. E., Liu X. M., Boska M. D., Lele S. M., Thiele G. M., Mikuls T. R., Dou H., Goldring S. R., Wang D.: Development of a macromolecular prodrug for the treatment of inflammatory arthritis: mechanisms involved in arthrotropism and sustained therapeutic efficacy. Arthritis Res Ther, 12 (2010) R170.

36. Quan L. D., Yuan F., Liu X. M., Huang J. G., Alnouti Y., Wang D.: Pharmacokinetic and biodistribution studies of N-(2-hydroxypropyl)methacrylamide copolymer-dexamethasone conjugates in adjuvant-induced arthritis rat model. Mol Pharm, 7 (2010) 1041-1049.

37. Yuan F., Nelson R. K., Tabor D. E., Zhang Y., Akhter M. P., Gould K. A., Wang D.: Dexamethasone prodrug treatment prevents nephritis in lupus-prone (NZB x NZW)F1 mice without causing systemic side effects. Arthritis Rheum, 64 (2012) 4029-4039.

38. Wang D., Miller S. C., Liu X. M., Anderson B., Wang X. S., Goldring S. R.: Novel dexamethasone-HPMA copolymer conjugate and its potential application in treatment of rheumatoid arthritis. Arthritis Res Ther, 9 (2007) R2.

39. Jensen K. D., Kopeckova P., Kopecek J.: Antisense oligonucleotides delivered to the lysosome escape and actively inhibit the hepatitis B virus. Bioconjug Chem, 13 (2002) 975-984.

40. Chipman S. D., Oldham F. B., Pezzoni G., Singer J. W.: Biological and clinical characterization of paclitaxel poliglumex (PPX, CT-2103), a macromolecular polymer-drug conjugate. Int J Nanomedicine, 1 (2006) 375-383.

41. Paz-Ares L., Ross H., O'Brien M., Riviere A., Gatzemeier U., Von Pawel J., Kaukel E., Freitag L., Digel W., Bischoff H., Garcia-Campelo R., Iannotti N., Reiterer P., Bover I., Prendiville J., Eisenfeld A. J., Oldham F. B., Bandstra B., Singer J. W., Bonomi P.: Phase III trial comparing paclitaxel poliglumex vs docetaxel in the second-line treatment of non-small-cell lung cancer. Br J Cancer, 98 (2008) 1608-1613.

42. Barinka C., Rinnova M., Sacha P., Rojas C., Majer P., Slusher B. S., Konvalinka J.: Substrate specificity, inhibition and enzymological analysis of recombinant human glutamate carboxypeptidase II. J Neurochem, 80 (2002) 477-487.

43. Mesters J. R., Barinka C., Li W., Tsukamoto T., Majer P., Slusher B. S., Konvalinka J., Hilgenfeld R.: Structure of glutamate carboxypeptidase II, a drug target in neuronal damage and prostate cancer. EMBO J, 25 (2006) 1375-1384.

44. Pinto J. T., Suffoletto B. P., Berzin T. M., Qiao C. H., Lin S., Tong W. P., May F., Mukherjee B., Heston W. D.: Prostate-specific membrane antigen: a novel folate hydrolase in human prostatic carcinoma cells. Clin Cancer Res, 2 (1996) 1445-1451.

45. Robinson M. B., Blakely R. D., Couto R., Coyle J. T.: Hydrolysis of the brain dipeptide N-acetyl-L-aspartyl-L-glutamate. Identification and characterization of a novel N-acetylated alpha-linked acidic dipeptidase activity from rat brain. J Biol Chem, 262 (1987) 14498-14506.

46. Carter R. E., Feldman A. R., Coyle J. T.: Prostate-specific membrane antigen is a hydrolase with substrate and pharmacologic characteristics of a neuropeptidase. Proc Natl Acad Sci U S A, 93 (1996) 749-753.

47. Chang S. S., Reuter V. E., Heston W. D., Bander N. H., Grauer L. S., Gaudin P. B.: Five different anti-prostate-specific membrane antigen (PSMA) antibodies confirm PSMA expression in tumor-associated neovasculature. Canc Res, 59 (1999) 3192-3198.

48. Silver D. A., Pellicer I., Fair W. R., Heston W. D., Cordon-Cardo C.: Prostate-specific membrane antigen expression in normal and malignant human tissues. Clin Cancer Res, 3 (1997) 81-85.

49. Perner S., Hofer M. D., Kim R., Shah R. B., Li H., Moller P., Hautmann R. E., Gschwend J. E., Kuefer R., Rubin M. A.: Prostate-specific membrane antigen expression as a predictor of prostate cancer progression. Hum Pathol, 38 (2007) 696-701.

50. Chang S. S., O'Keefe D. S., Bacich D. J., Reuter V. E., Heston W. D., Gaudin P. B.: Prostate-specific membrane antigen is produced in tumor-associated neovasculature. Clin Cancer Res, 5 (1999) 2674-2681.

51. Liu H., Moy P., Kim S., Xia Y., Rajasekaran A., Navarro V., Knudsen B., Bander N. H.: Monoclonal antibodies to the extracellular domain of prostate-specific membrane antigen also react with tumor vascular endothelium. Cancer research, 57 (1997) 3629-3634.

52. Rajasekaran A. K., Anilkumar G., Christiansen J. J.: Is prostate-specific membrane antigen a multifunctional protein? Am J Physiol Cell Physiol, 288 (2005) C975-981.

53. Hinkle G. H., Burgers J. K., Neal C. E., Texter J. H., Kahn D., Williams R. D., Maguire R., Rogers B., Olsen J. O., Badalament R. A.: Multicenter radioimmunoscintigraphic evaluation of patients with prostate carcinoma using indium-111 capromab pendetide. Cancer, 83 (1998) 739-747.

54. Lopes A. D., Davis W. L., Rosenstraus M. J., Uveges A. J., Gilman S. C.: Immunohistochemical and pharmacokinetic characterization of the site-specific immunoconjugate CYT-356 derived from antiprostate monoclonal antibody 7E11-C5. Canc Res, 50 (1990) 6423-6429.

55. Liu H., Rajasekaran A. K., Moy P., Xia Y., Kim S., Navarro V., Rahmati R., Bander N. H.: Constitutive and antibody-induced internalization of prostate-specific membrane antigen. Canc Res, 58 (1998) 4055-4060.

56. Rajasekaran S. A., Anilkumar G., Oshima E., Bowie J. U., Liu H., Heston W., Bander N. H., Rajasekaran A. K.: A novel cytoplasmic tail MXXXL motif mediates the internalization of prostate-specific membrane antigen. Mol Biol Cell, 14 (2003) 4835-4845.

57. Adair J. R., Howard P. W., Hartley J. A., Williams D. G., Chester K. A.: Antibody-drug conjugates - a perfect synergy. Expert Opin Biol Ther, 12 (2012) 1191-1206.

58. Wu L. Y., Liu T., Grimm A. L., Davis W. C., Berkman C. E.: Flow cytometric detection of prostate tumor cells using chemoaffinity labels. Prostate, 71 (2011) 52-61.

59. Liu T., Nedrow-Byers J. R., Hopkins M. R., Wu L. Y., Lee J., Reilly P. T., Berkman C. E.: Targeting prostate cancer cells with a multivalent PSMA inhibitor-guided streptavidin conjugate. Bioorg Med Chem Lett, 22 (2012) 3931-3934.

60. Brik A., Wong C. H.: HIV-1 protease: mechanism and drug discovery. Org Biomol Chem, 1 (2003) 5-14.

61. Davies D. R.: The structure and function of the aspartic proteinases. Annu Rev Biophys Biophys Chem, 19 (1990) 189-215.

62. Kohl N. E., Emini E. A., Schleif W. A., Davis L. J., Heimbach J. C., Dixon R. A., Scolnick E. M., Sigal I. S.: Active human immunodeficiency virus protease is required for viral infectivity. Proc Natl Acad Sci U S A, 85 (1988) 4686-4690.

63. Prabu-Jeyabalan M., Nalivaika E., Schiffer C. A.: Substrate shape determines specificity of recognition for HIV-1 protease: analysis of crystal structures of six substrate complexes. Structure, 10 (2002) 369-381.

64. Konvalinka J., 2013, Personal Communication.

65. Wensing A. M., van Maarseveen N. M., Nijhuis M.: Fifteen years of HIV Protease Inhibitors: raising the barrier to resistance. Antiviral Res, 85 (2010) 59-74.

66. Rezacova P., Pokorna J., Brynda J., Kozisek M., Cigler P., Lepsik M., Fanfrlik J., Rezac J., Grantz Saskova K., Sieglova I., Plesek J., Sicha V., Gruner B., Oberwinkler H., Sedlacek J., Krausslich H. G., Hobza P., Kral V., Konvalinka J.: Design of HIV protease inhibitors based on inorganic polyhedral metallacarboranes. J Med Chem, 52 (2009) 7132-7141.

67. Kozisek M., Bray J., Rezacova P., Saskova K., Brynda J., Pokorna J., Mammano F., Rulisek L., Konvalinka J.: Molecular analysis of the HIV-1 resistance development: enzymatic activities, crystal structures, and thermodynamics of nelfinavir-resistant HIV protease mutants. J Mol Biol, 374 (2007) 1005-1016.

68. Williams J. W., Morrison J. F.: The kinetics of reversible tight-binding inhibition. Methods Enzymol, 63 (1979) 437-467.

69. Masa M., Maresova L., Vondrasek J., Horn M., Jezek J., Mares M.: Cathepsin D propeptide: mechanism and regulation of its interaction with the catalytic core. Biochemistry, 45 (2006) 15474-15482.

70. Tykvart J., Navratil V., Sedlak F., Corey E., Colombatti M., Fracasso G., Koukolik F., Barinka C., Sacha P., Konvalinka J.: Comparative analysis of monoclonal antibodies against prostate-specific membrane antigen (PSMA). Prostate, 74 (2014) 1674-1690.

71. Tykvart J., Sacha P., Barinka C., Knedlik T., Starkova J., Lubkowski J., Konvalinka J.: Efficient and versatile one-step affinity purification of in vivo biotinylated proteins: expression, characterization and structure analysis of recombinant human glutamate carboxypeptidase II. Protein Expr Purif, 82 (2012) 106-115.

72. Bradford M. M.: A rapid and sensitive method for the quantitation of microgram quantities of protein utilizing the principle of protein-dye binding. Anal Biochem, 72 (1976) 248-254.

73. Sacha P., Zamecnik J., Barinka C., Hlouchova K., Vicha A., Mlcochova P., Hilgert I., Eckschlager T., Konvalinka J.: Expression of glutamate carboxypeptidase II in human brain. Neuroscience, 144 (2007) 1361-1372.

74. Šubr V., Kostka L., Strohalm J., Etrych T., Ulbrich K.: Synthesis of Well-Defined Semitelechelic Poly[N-(2-hydroxypropyl)methacrylamide] Polymers with Functional Group at the α-End of the Polymer Chain by RAFT Polymerization. Macromolecules, 46 (2013) 2100-2108.

75. Šubr V., Ulbrich K.: Synthesis and properties of new N-(2-hydroxypropyl)methacrylamide copolymers containing thiazolidine-2-thione reactive groups. Reactive and Functional Polymers
66 (2006) 1525-1538.

76. Tykvart J., Schimer J., Barinkova J., Pachl P., Postova-Slavetinska L., Majer P., Konvalinka J., Sacha P.: Rational design of urea-based glutamate carboxypeptidase II (GCPII) inhibitors as versatile tools for specific drug targeting and delivery. Bioorg Med Chem, 22 (2014) 4099-4108.

77. Fanfrlik J., Bronowska A. K., Rezac J., Prenosil O., Konvalinka J., Hobza P.: A reliable docking/scoring scheme based on the semiempirical quantum mechanical PM6-DH2 method accurately covering dispersion and H-bonding: HIV-1 protease with 22 ligands. J Phys Chem B, 114 (2010) 12666-12678.

78. Huang Z., Hwang P., Watson D. S., Cao L., Szoka F. C., Jr.: Tris-nitrilotriacetic acids of subnanomolar affinity toward hexahistidine tagged molecules. Bioconjug Chem, 20 (2009) 1667-1672.

10. Appendix

Following supplementary figures depict the molecular structure of iBodies used in this thesis.

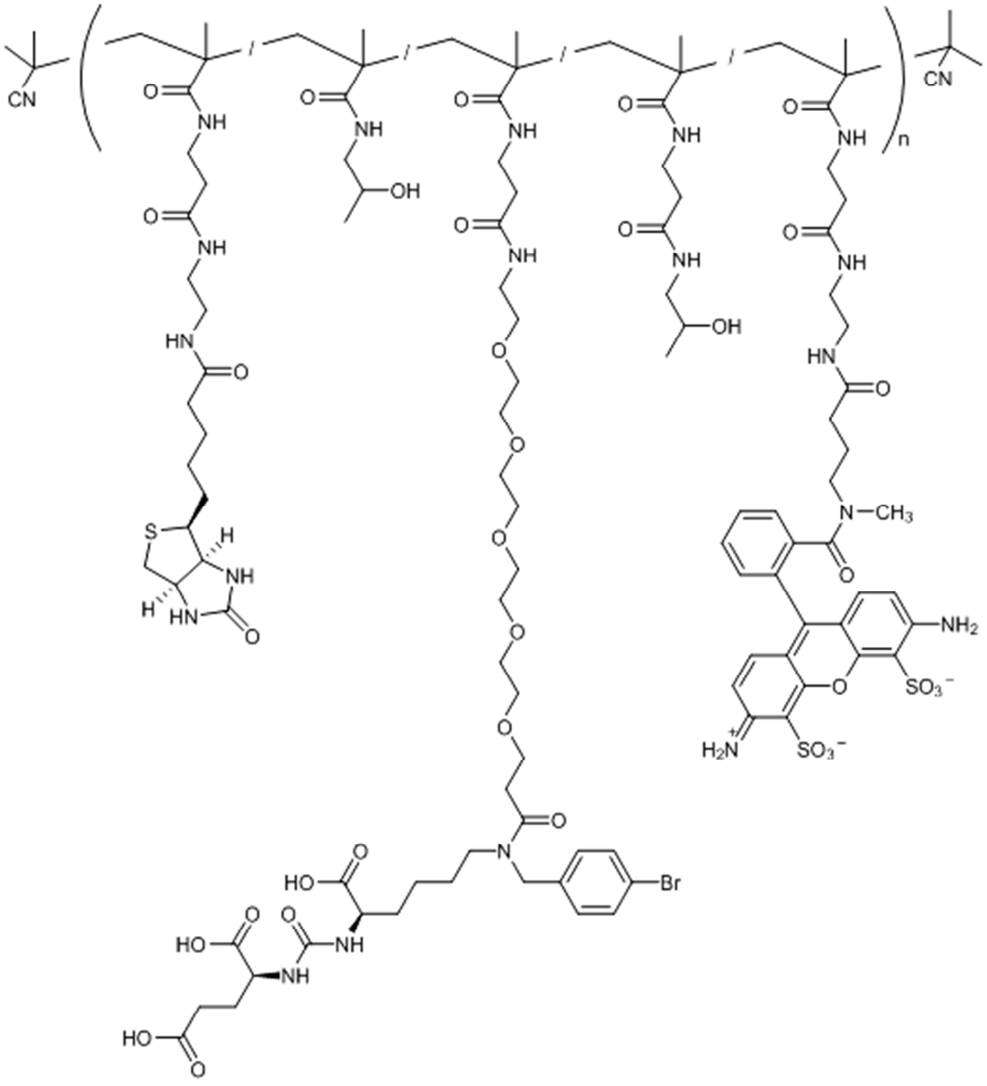

Supplementary figure 1: Structure of iBody 1. iBody 1, targeting GCPII, contains Compound **1** (GCPII inhibitor), ATTO 488, and biotin.

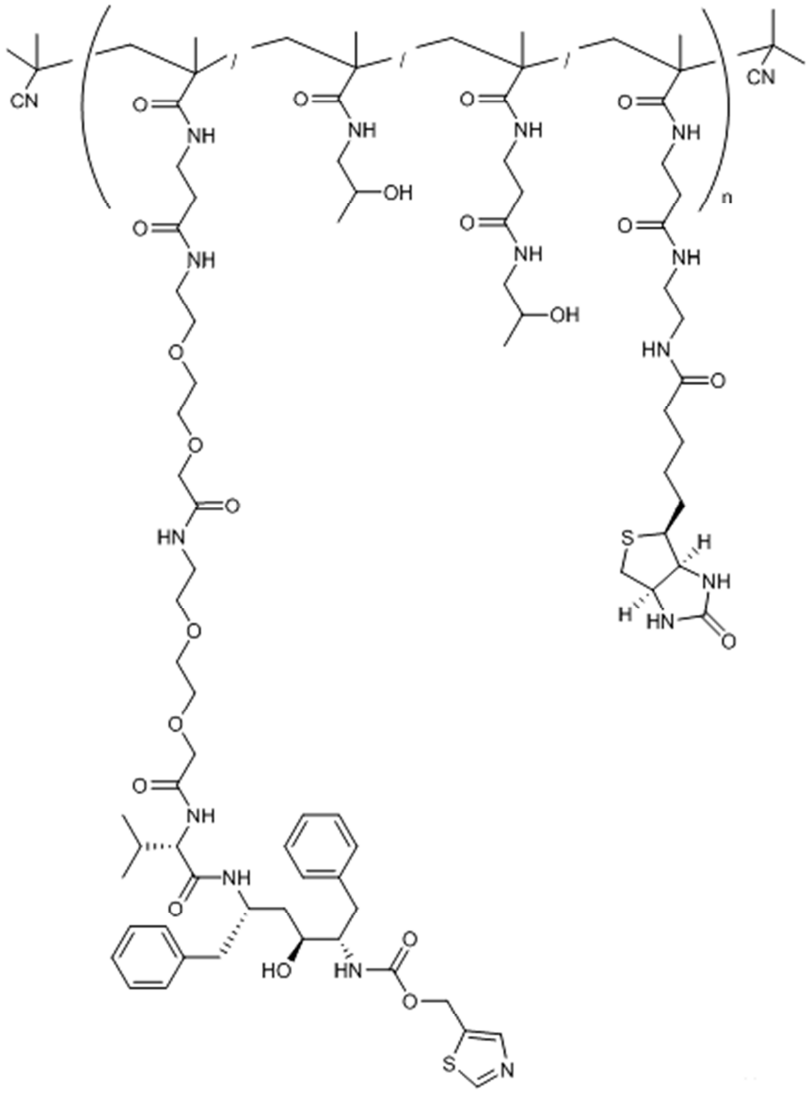

Supplementary figure 2: Structure of iBody 2. iBody 2, targeting HIV-1 protease, contains Compound **2** (a derivative of an HIV-1 protease inhibitor ritonavir), and biotin.

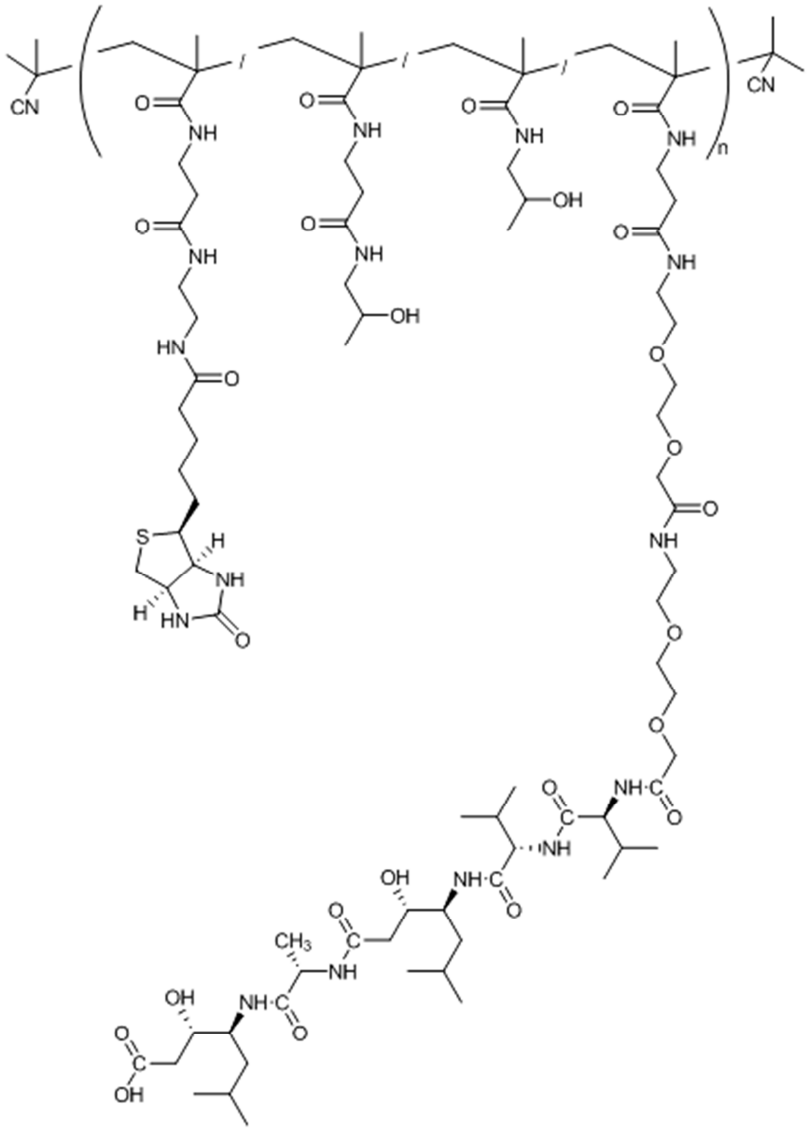

Supplementary figure 3: Structure of iBody 3. iBody 3, targeting aspartic proteases, contains Compound **3** (a derivative of an aspartic proteases inhibitor pepstatin A), and biotin.

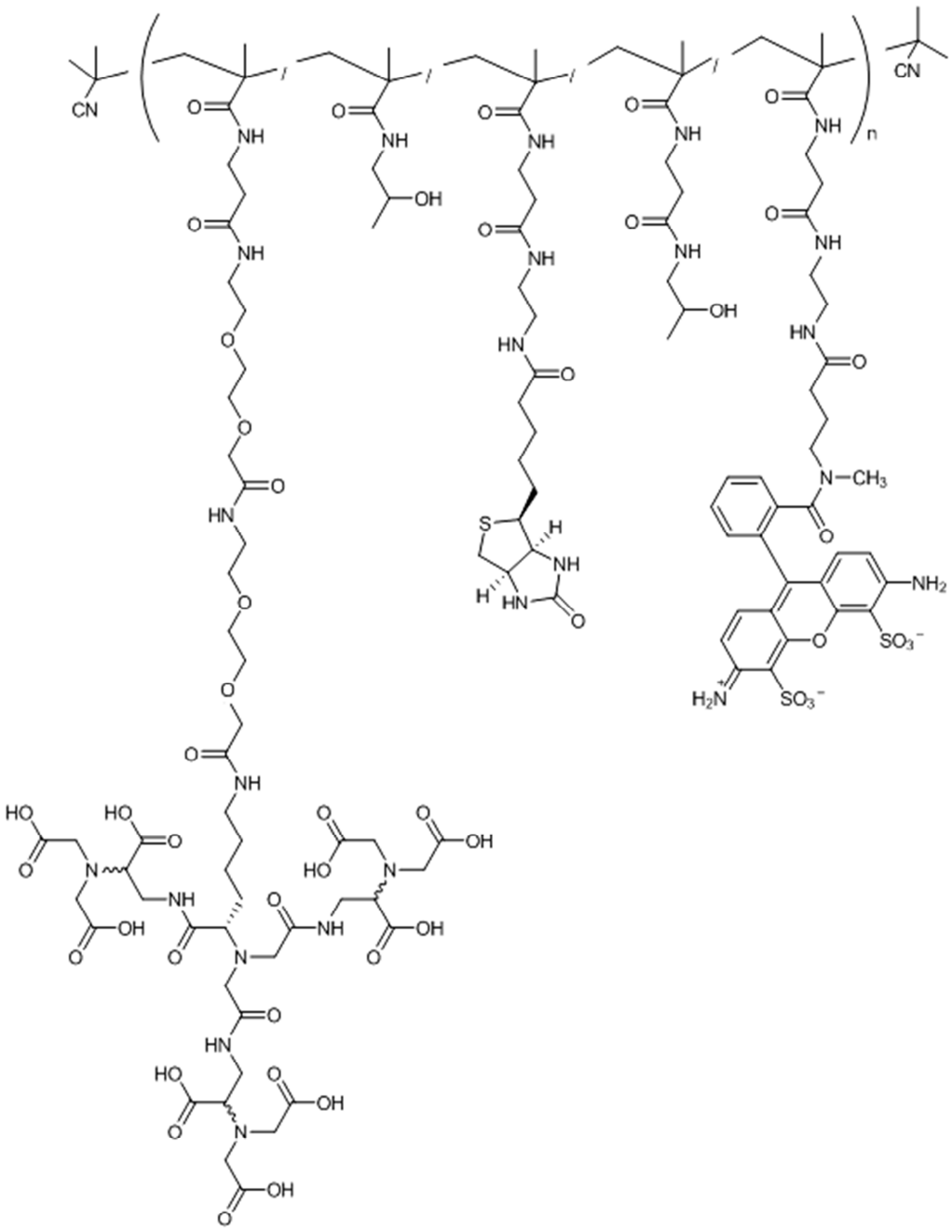

Supplementary figure 4: Structure of iBody 4. iBody 4, targeting His-tagged proteins, contains Compound **4** (a derivative of a nitrilotriacetic acid), biotin, and ATTO 488.

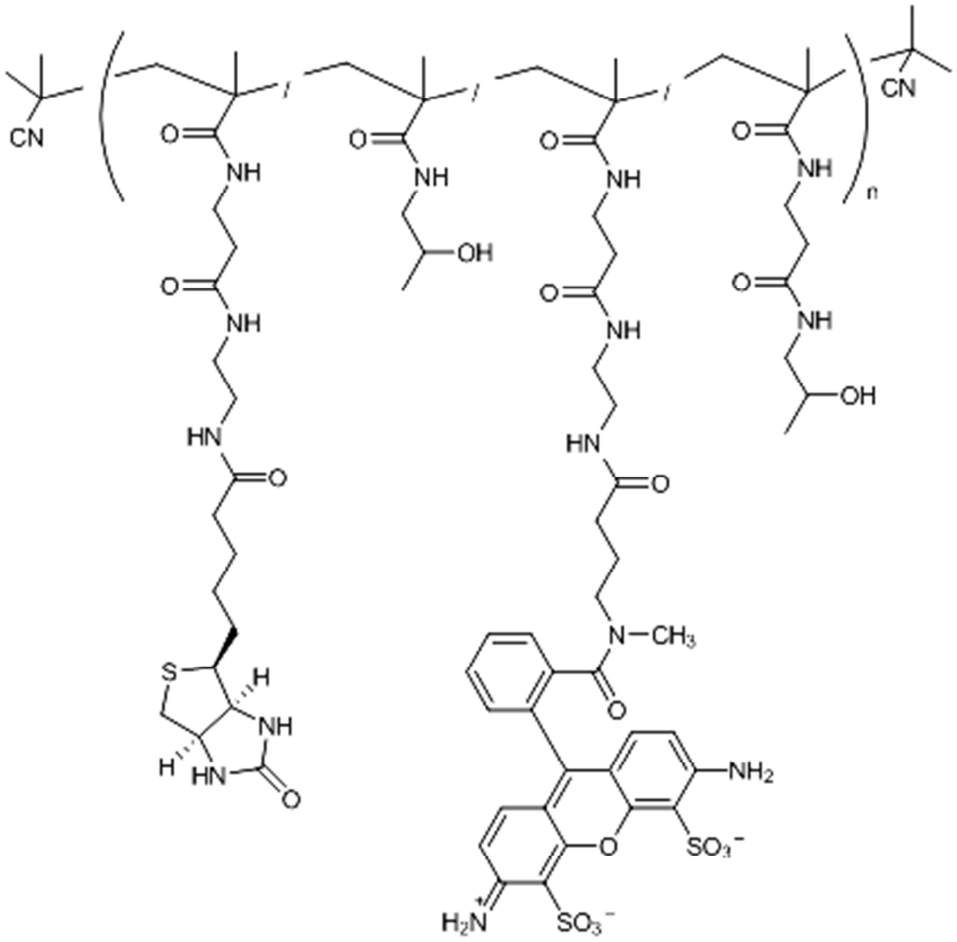

Supplementary figure 5: Structure of iBody 5. iBody 5, serving as a negative control for iBodies 1 and 4,contains biotin and ATTO 488.

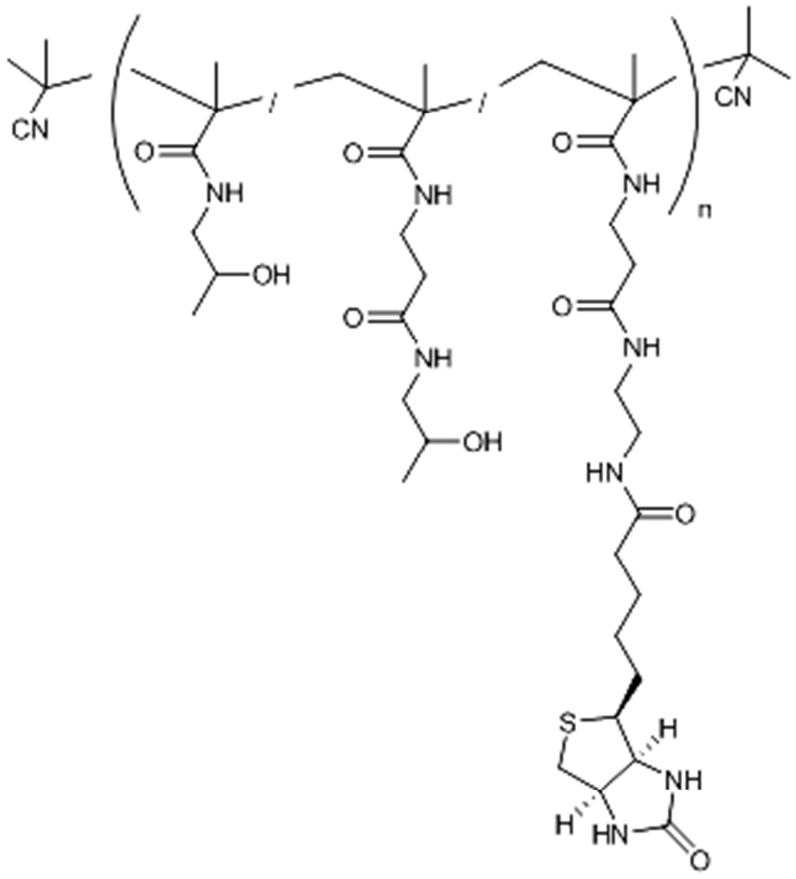

Supplementary figure 6: Structure of iBody 6. iBody 6, serving as a negative control for iBodies 2 a 3, contains only biotin.

Svoluji k zapůjčení této práce pro studijní účely a prosím, aby byla řádně vedena evidence vypůjčovatelů.

Jméno a příjmení s adresou	Číslo OP	Datum vypůjčení	Poznámka